Finite Element Modelling of a Sustainable Hybrid Natural Fibre Sandwich Panel Under Bending

A dissertation submitted by

Iman Farahbakhsh

Supervised by Associate Professor Yan.Zhuge

ERP2016: Engineering Research Project 2015

For the degree:

Bachelor of Engineering (Civil)

Abstract

Mass production of houses on a large scale at an affordable price, acceptable quality and sustainable method has always been one of the challenges for the public and private sector. Applying natural fibre reinforced composite panels in the modular building is one of the promising approaches to this challenge. This project modelled and analysed jute, hemp and MDF fibre reinforced composite panels under flexural loading using Strand7 computer software.

It was found that the introduction of the intermediate layer of jute, hemp and MDF improved the load carrying capacity of conventional insulated panels. However, panels with jute fibre displayed less stiffness that could be a point of concern for practical applications. Experimental results indicated that delamination and debonding between the core and intermediate layers have been a major failure cause of hybrid sandwich panels. It was understood that modelling delamination between layers was fairly complex and required significantly more time which was out of the scope of this project. Therefore, modelling and analysing the bonding agent in sandwich panels is suggested for further work in the future.

University of Southern Queensland

Faculty of Health, Engineering and Sciences

ENG4111/ENG4112

Research Project

Limitations of Use

The Council of the University of Southern Queensland, its Faculty of Health, Engineering & Sciences, and the staff of the University of Southern Queensland, do not accept any responsibility for the truth, accuracy or completeness of material contained within or associated with this dissertation.

Persons using all or any part of this material do so at their own risk, and not at the risk of the Council of the University of Southern Queensland, its Faculty of Health, Engineering & Sciences or the staff of the University of Southern Queensland.

This dissertation reports an educational exercise and has no purpose or validity beyond this exercise. The sole purpose of the course pair entitled "Research Project" is to contribute to the overall education within the student's chosen degree program. This document, the associated hardware, software, drawings, and other material set out in the associated appendices should not be used for any other purpose: if they are so used, it is entirely at the risk of the user.

University of Southern Queensland

Faculty of Health, Engineering and Sciences

ENG4111/ENG4112 Research Project

Certification of Dissertation

I certify that the ideas, designs and experimental work, results, analyses and conclusions set out in this dissertation are entirely my own effort, except where otherwise indicated and acknowledged. I further certify that the work is original and has not been previously submitted for assessment in any other course or institution, except where specifically stated.

I. Farahbakhsh

0061075278

_____

Date: _12_/_10_/_2016_

Acknowledgement

This project was supervised by Associate Professor Yan Zhuge and I would like to thank her for her tireless support and guidance. She has assisted me constantly throughout the year towards the completion of the project with sharing her invaluable knowledge and experience. I was fortunate to work under her supervision. I would also like to thank my family and friends for their support and patience that helped me a lot to go through the end of this project.

Table of Contents

Table of Figures

List of Tables

1 Introduction

Providing quality affordable accommodation in a sustainable construction method has always been of major challenges facing the housing industry. Prefabricated or modular panelised construction is a method in which house components or parts are pre-fabricated at factory in and transported and erected on site. Modular panelised system is able to reduce construction duration and labour cost. Consequently, more houses can be built considerably faster with lower prices. Other advantages are such as the reduction or elimination of costing delays, less weather damage to material, utilization of precisely engineered material, less amount of energy for cooling and heating and enhanced insulation. Modular panelised systems conventionally use structural insulated panels (SIPs) as favourable construction material. Composite sandwich structure with soft rigid expanded polystyrene core has been broadly utilised in building industry in recent decade particularly after the Modular panelised construction gained considerable attention in the housing market.

Structural insulated panel (SIP), shown in Figure 1.1 is composed of two skin layers of metal (Steel or aluminium) and a soft rigid polystyrene core in the middle with a variety of thicknesses. SIPs are known as sandwich panels due to their shape which resembles a sandwich. Metal skins are one of the best choices for the outer layer for many reasons however the price has always been a concern. Therefore, reducing the thickness of the outer layers can reduce the cost of manufacturing SIPs. However, reducing the thickness of the layer results in face wrinkling and proneness to structural loading.

A practical and sustainable solution to this problem is adding an intermediate layer of natural fibre reinforced plastic (NFRP) to the conventional insulated panels to creates Hybrid Sandwich Panels. Natural fibres are of major renewable resources in the construction industry and have numerous advantages such as being environmentally friendly, flood resistance and higher strength over typical SIPs. However, it is crucial to design and analyse sandwich panels under structural loading before

applying them in industry. The structural behaviour of hybrid sandwich panels under bending can be analysed using finite element method in computer software.

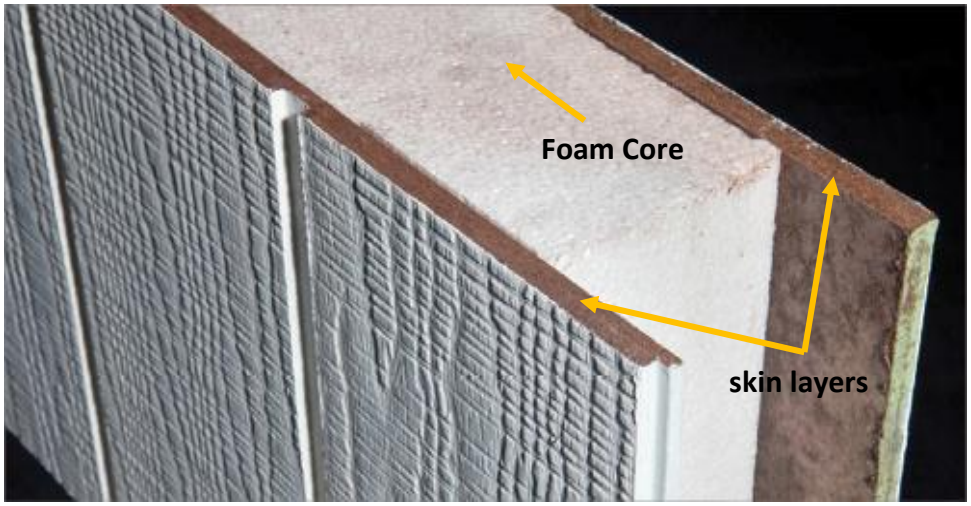

Figure 1.1: Structural insulated panel (SIP)

Source: http://www.yourhome.gov.au/

1.1. Project Background

Composite panels were initially used in aerospace and aircraft industry due to their ease of construction, low weight and high strength under loading. These properties enabled the industry to build lighter aircraft which required smaller engines and higher efficiency. After successful application of sandwich panels in the aircraft industry, other fields including building industry were encouraged to use composite material for a variety of applications. Therefore, the behaviour of composite panels under structural loading and climatic situations was required to be well understood for design purposes. Moreover, strengthening composite panels by using alternative materials became a significant research field. However, with increasing environmental concerns in recent decades, environmentally friendly material and sustainable methods of construction have become highly in demand. This brought natural fibres as one of the most favourable material to be used in the construction industry due to their vast availability and biodegradability.

1.2. Project Aims

A computer generated model for analysing the application of natural fibres on insulated panels enables researchers to estimate the behaviour of structural insulated panels reinforced with different types of natural fibres with various thicknesses at a significantly lower cost and reduced time. On this basis, the aim of this project is to provide a 3D model for analysing the application of natural fibres on structural insulated panels under bending.

Requirements of this project are listed as:

- Reproduce 3D models of the panels in Strand7
- Test the 3D models under bending and record the data
- Compare the data against experimental results from Dr. Fajrin
- Analyse the results and comment on accuracy and applicability of models for analysing other types hybrid panels

1.3. Constraints

Natural fibres are of different types and thicknesses thus, it was decided to limit the generated model to two most used types in the construction industry; jute and hemp fibres. This selection not only provides a better scope of works for an undergraduate level but also represents two natural fibres with the best performance for construction purposes among other NFRPs. The project is also constrained to modelling and analysing the behaviour of reinforced SIPs under bending. Therefore, the analysis of panels under tension, compression, buckling, shear and torsion will not be considered in this project. Furthermore, face sheet is limited to aluminium and foam core to Expanded Polystyrene (EPS) for SIP in this project.

Despite these limitations, the process and details of creating the model can be used by other researchers for other load types in the future.

1.4. Project objectives

The following objectives are set for this project:

- To produce a 3D finite element model using Strand7 for analysing the application of NFRP on SIP
- To plot graphs showing load versus deflection for various types of NFRP and thicknesses
- To validate the obtained load-deflection curves by comparing them with the graphs from the real experiment
- To conduct a parametric study to evaluate the influence of parameters such as width, thickness and type of natural fibre on SIP

2 Background and literature review

2.1 Introduction

Since 1935, many studies have been undertaken to analyse and learn the behaviour of composite panels under loading and climatic conditions. Most of these studies were done in a laboratory and by real specimens. It was only after the development of the finite element modelling computer programs that modelling structural insulated panels initiated.

This section reviews the information regarding sandwich panels from previous papers and outlines the experimental conditions and methodology from Fajrin et al. (2013a) in order to provide a scale for validating results from the computer program.

2.2 Performance of SIP

2.2.1 Structural insulated panels

Structural insulated panel (SIP) is a structural member constructed from two skin layers with a rigid relatively thick foam core in the middle which has been utilised as wall, roof and floor in the prefabricated housing for years. The core carries the shear loads and stabilises the structure against bulking and wrinkling and face sheets carry bending stresses. It was first introduced in 1935 in the United States as a response to high level of market demand for faster and more economical method of construction. Due to the significantly low amount of wastage and enabling fast-paced construction, it has been favourable in building industry as walls, floors and slabs (Abang Abdullah Abang, Mohammad & Yen Lei 2013). Moreover, ease of transportation, low maintenance, good insulation, high level of strength to weight ratio and ease of replacement for repair purposes makes structural composite panels an ideal choice in the building industry.

The main components of structural panels are thick core, extra thin adhesive and thin faces or skins. The adhesive or bonding agent provides connection and transfers shear between the core and skins. The core contributes to the high section modulus of the panel and takes care of the applied shear force (Davies, 2001).

Common types of SIP face sheet include oriented strand board (OSB) which is a wood base board, fibre reinforced polymer (FRP), aluminium and steel, cement board and calcium silicate board (Abang Abdullah Abang, Mohammad & Yen Lei 2013). In fact, a thin layer of almost any material can be used as skin layers of composite panels which makes the use of panels favourable in many situations and a variety of applications. However, it should be taken into account that some types of cores and bonding agents are not compatible and will result in a chemical reaction and hence, instant failure of the panel (Zenkert, 1995).

Due to their special configuration, composite panels have their own weak points which according to Mostafa et al. (2013), are known as face wrinkling and failure due to shear stress. Various research has been undertaken (Zhou & Stronge, 2005; Grenestedt & Reany, 2007) in order to introduce and analyse different approaches to strengthening composite panels. Some of these approaches are introducing shear keys, enhanced skins and adhesives and direction of fibres in panels.

Furthermore, the cost of using SIP in construction has always been a concern. The cost of using SIPs still can be reduced by decreasing the thickness of skin layers although, thinner skin can cause wrinkling and lessened structural stiffness of the panel. To overcome this challenge, an intermediate layer with relatively large tensile strength such as natural fibre reinforced polymers can be added to SIPs to increase the panel strength under structural loading (Fajrin et al. 2013a).

Increasing environmental concerns and global consciousness toward the natural resource preservation has attracted numerous researchers into the application of Natural fibre reinforced polymer (NFRP) in lieu of synthetic fibres in building industry as cost effective bio-composites. NFRP advantages are their low cost, high strength, low density, bio-degradability, environmentally friendly, non-corrosiveness and renewability. Natural fibres are available as coconut fibre (coir), jute, palm, hemp, abaca, sisal, bamboo, wood and paper in their natural condition (Herrera-Franco & Valadez-González 2004).

2.2.2 Performance of sandwich panels under bending load

A study (Fajrin et al. 2013a) illustrates the flexural behaviour of a conventional SIP, without any NFRP intermediate layer, under bending stress. This specimen is chosen as a control specimen in order to demonstrate the effect of applying an intermediate layer to SIP. It is noticed that the control specimen fails under an average load of 328 N. This is expected to be achieved in the computer generated model.

The results from previous studies (Fajrin et al. 2013a) shows that reinforcing SIP with NFRP can increase its flexural strength up to 40% for jute layer and 95% for hemp layer. It is realised that ultimate flexural strength is highly dependent on the type and thickness of the NFRP applied as an intermediate layer (Fajrin, Zhuge, Bullen &Wang 2013b). These values of flexural strength for reinforced panel specimens are expected to be obtained in the numerical model.

In testing SIPs, the bending load is applied to a monolithic panel attached to a homogeny material. The resulting stress distribution is a straight sloping plain that has a remarkable transform at the top and bottom interface where skin layers and core meet each other. This large inconsistency in stress distribution is the main cause of failure in an early stage in sandwich panel structures. Introducing an intermediate layer with median mechanical properties between the skin and core is to reduce this gap which is illustrated in Figure 2.1.

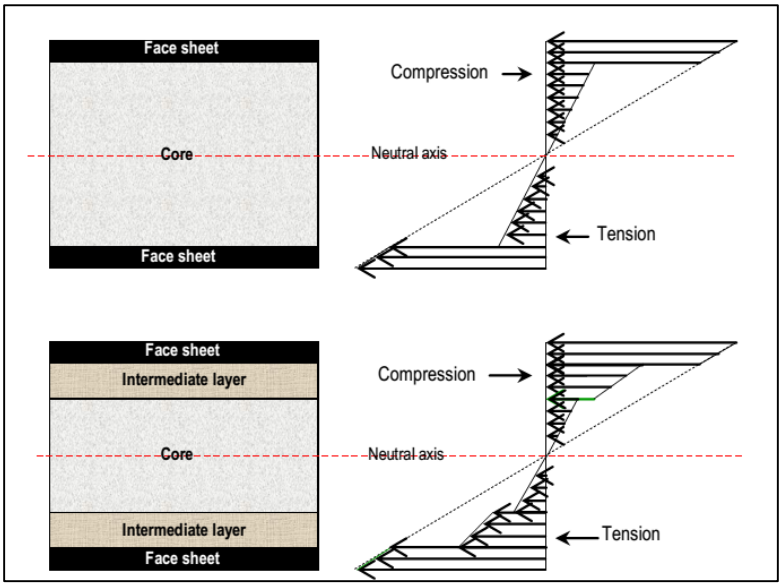

Figure 2.1: Stress distribution in SIP before and after application of NFRP

Source: (Fajrin et al. 2013b)

According to the Hook's law, for all materials, stress is a function of their modulus of elasticity. The selected intermediate layer should have a modulus of elasticity between the skin layer and the core to reduce the large difference between modulus of elasticity of skin and core. However, the mechanism of the failure of the sandwich panel under bending load is a considerably complex incident. Previous studies (Mamalis, Spentzas, Manolakos, Pantelelis &Ioannidis 2008; Steeves & Fleck 2004) have evaluated, tested and developed equations to analyse the failure mechanism of SIPs under bending load. These equations are summarised in (Fajrin et al. 2013b) as follows:

Face micro-buckling $$:\frac{P}{b} = \frac{4t_f t_c \sigma f}{L} \quad (2.1)$$

Face wrinkling $$:\frac{P}{b} = \frac{2t_f t_c}{L} \sqrt[3]{E_f E_c G_c} \quad (2.2)$$

Core shear $$:\frac{P}{b} = 2t_c \tau_c \quad (2.3)$$

Indentation $$:\frac{P}{b} = \sqrt[3]{\frac{\pi^2 E_f \sigma_c^2 t_f^3 t_c}{L}} \quad (2.4)$$

Where:

τ_c =shear strength

σ_c = compressive strength

b =width of the sandwich panel

E= elastic modulus

G =Foam core shear modulus

L =span between supports

P = load

t = thickness of the layer

f = face sheet

c =core

I=internal layer

Theoretical deflections of sandwich panels can be calculated using ASTM C 393-00 (ASTM, 2000), the standard test method for flexural properties of sandwich constructions. According to this standard, the total deflection of a sandwich panel equals the sum of the deflection of all layers in bending and shear. Total deflection under two-point load at one-quarter span can be calculated as:

$$\Delta = \frac{11\mathrm{PL}^3}{768\mathrm{D}} + \frac{\mathrm{PL}}{8\mathrm{U}} \quad (2.5)$$

Where:

D = The stiffness in $\mathrm{N.mm}^2$

U = panel shear rigidity

P = Load (N)

L = Span length (mm)

However, the above equation could not be used for this project as the loading configuration was different.

Roylance (2000) suggested a general equation for calculating deflection of sandwich panels as:

$$\delta(x) = \frac{P(L-a)}{6LEI}\left[\frac{L}{L-a}(x-a)^3 - x^3 + (L^2 - (L-a)^2 x)\right] + \frac{Pa}{6LEI}\left[\frac{L}{a}(x-(L-a))^3 - x^3 + (L^2 - a^2)x\right] \quad (2.6)$$

For this project, $a = \frac{L}{3}$ and $x = \frac{L}{2}$ therefore,

$$\delta = \frac{23PL^3}{1296EI} \quad (2.7)$$

This equation can be rearranged as:

$$\delta = \frac{23PL^3}{1296(EI)_{eq}} \quad (2.8)$$

It is noted that when a low-density core is used as the core of the sandwich panel, shear deflection is a major factor to be taken into account for deflection calculation. The mechanism of deformation under four-point loading is shown in Figure 2.2.

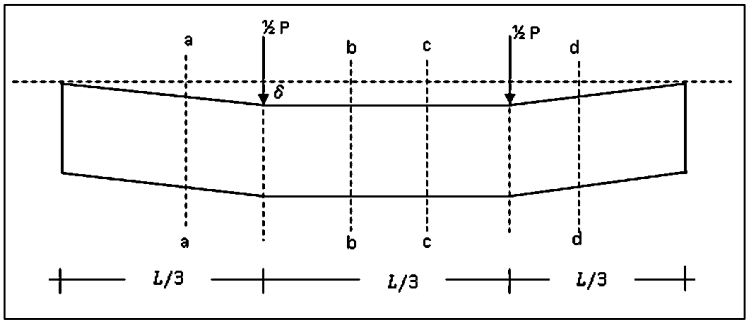

Figure 2.2: Deformation under four-point loading

The deflection in the point of load exertion on the panel is presented as:

$$\frac{\delta}{\frac{L}{3}} = \gamma = \frac{Q}{G_c bd} \tag{2.9}$$

$$\delta = \frac{\frac{QL}{3}}{G_c bd} \tag{2.10}$$

$$Q = \frac{P}{2} \tag{2.11}$$

$$\delta = \frac{\frac{P}{2} \cdot \frac{L}{3}}{G_c bd} \tag{2.12}$$

$$\delta = \frac{PL}{6(G_c bd)} \tag{2.13}$$

$$\delta = \frac{PL}{6(AG)_{eq}} \tag{2.14}$$

Therefore, the total deflection of the sandwich panel under four-point load can be described as a linear superposition of the deformation of the panel caused by bending and shear. Manalo (2009) stated that deflection of sandwich panels under bending load can be calculated as:

$$\delta = \frac{23PL^3}{1296(EI)_{eq}} + \frac{PL}{6(AG)_{eq}} \tag{2.15}$$

Shear modulus of core is calculated as:

$$G_c = \frac{E}{2(1+V)} \tag{2.16}$$

Somayaji (1995) indicated that measuring shear modulus of the core through experiment is tedious and he recommended the above calculation as well. The bending stiffness of each sandwich panel can be calculated using equation.

2.3 Numerical modelling of SIPs

In order to have a better understanding of what is involved in modelling a structural panel, some research is undertaken in previous studies (Hidallana-Gamage, Thambiratnam & Perera 2014; Mousa & Uddin 2012; Ramroth et al., 2015). A generic approach indicates that skin layers and foam core should be 3D modelled separately to compose an element. Eight nodes and three degrees of freedom are introduced to each plate with translations into x, y and z directions. Plasticity, creep, swelling, deflection

and strain are defined for the element. It should be taken into account that both skin layers and core in SIP act identically in all directions whereas the NFRP layer acts in two directions (Mousa & Uddin 2012). Therefore, face sheets and core are modelled as isotropic (same grain in each direction) while NFRP layers are modelled as an orthotropic material. Properties such as modulus of elasticity, tensile strength and percentage of density and elongation for all materials in the model are required to be defined in three planes. Loading and boundary conditions and plane constraints for face sheets, NFRP layers and the core are defined and applied in accordance with the real experiment. Resulting graphs of load versus deflection is plotted by the software and compared with the real experiment data.

2.3.1 General characteristics of Strand7

Strand7 is a finite element modelling software developed in Sydney, Australia and is known for linear and non-linear analysis, flexural, buckling and heat transfer modelling. It is widely used in construction and engineering industry in modelling new materials and composite application, the design of structures and analysis of existing infrastructure and buildings. (Strand7 2015).

2.3.2 Finite element modelling using Strand7

What makes it attractive to work with Strand7 is access to an unlimited number of nodes, elements and equations. This characteristic enables the operator to create precise models with a high level of details. Dynamic rotation of the model can be easily undertaken using Wireframe mode in this software and using mouse directions. ‘Group’ function can be utilised to manage large models to organise them into an intuitive model. User defined coordinate system, plate thickness render, sub-modelling and multiple freedom cases are just a few fascinating features of Strand7 (Strand7 2015).

2.4 Review of experimental methodology

Bending or flexural test generally includes bending a specimen until it fractures. During the test, load and corresponding deflection are recorded and compared to a control specimen. The largest load that a specimen is able to take before the fracture is called flexural strength or modulus of rupture. There are various methods that the flexural test can be conducted including three point and four point methods. Fajrin et al. (2013a) found that the best method of exerting load on sandwich panels in bending test is the four-point bending load. This fact is also verified by former researchers (Manalo et al. 2009).

Adding NFRP intermediate layer to structural insulated panels have been successfully tested at the University of Southern Queensland, Australia (Fajrin et al. 2013a). Accurate data is available and table of load versus deflection and strain for various configurations are plotted. The specimens for this experiment were classified as medium and large specimens. Medium ones were cut into a span of 450 mm and the length of 550 mm, width of 50 mm and thickness of 22 mm ($550 \times 50 \times 22$ mm). The skin layers were aluminium 5005 H34 sheet with a thickness of 0.5 mm on both sides of the EPS core. Jute and hemp intermediate layers were 3 mm thick and the thickness of the expanded polystyrene core for control specimen (without NFRP) are 15 mm and for two other specimen type (with jute and hemp intermediate layers) is 21 mm in order to maintain an overall thickness of 22 mm. In the real experiment, control medium specimen were named as CTR-SP, jute medium specimens as JFC-SP and hemp medium specimen as HFC-SP in order to make comparison purposes easier. The same method was followed in this project.

Control specimen at large scale were prepared at dimensions of ($1150\times 100 \times 52$ mm) with the span length of 900 mm. control specimen consist of a 50 mm EPS core with aluminium skins of 1.0 mm on both sides. Jute and MDF specimens at large size included an EPS core of 40 mm, intermediate natural fibre of 5 mm on both sides of the core and aluminium skins of 1.0 mm to keep overall thickness of 52 mm. Large scale specimens are known as CTR-SIP for control specimen, JFC-SIP for the specimen

with jute intermediate layer and MDF-SIP for the specimen with MDF intermediate layer. It is noticed that the large scale specimen is actually the smallest size of sandwich panels that are currently available in the market. Mechanical properties of aluminium and EPS, jute and hemp natural fires and specimens' configuration are shown in

Table 2.1, Table 2.2, Table 2.3 and Table 2.4 respectively.

Moreover, as the purpose of the project is to analyse the specimen non-linearly, it was vital to create the table of stress-strain for each material. Data points for each material is shown in

Table 2.1: Mechanical properties of Aluminium and EPS

Aluminium 5005 H34	
Physical and mechanical properties	
Density (ρ)	2700 kg/m^3
Modulus Elasticity (E)	68.2 GPa
Poisson ratio	0.33
Shear modulus	25.9 GPa
Shear strength	96.5 MPa
Ultimate tensile strength	159 MPa
Yield tensile strength	138 MPa
Isolite® EPS	
Physical and mechanical properties	
Grade	VH (Very High)
Density (ρ)	28 kg/m^3
Modulus Elasticity (E)	7250 kPa (7.25 MPa)
Poisson ratio	0.35
Flexural strength	337 kPa
Shear stress	240 kPa

Source: Fajrin et al. (2013a)

Table 2.2: Mechanical properties of JNC

Jute natural fibre composite-tensile, thickness (3-4 mm) – (JNC0-TSL)					
Specimen	**Area (mm^2)**	**Peak load (N)**	**Peak stress (MPa)**	**Modulus of elasticity (MPa)**	**Poisson's ratio (mm/mm)**
1	111.82	3128	27.97	5641	0.625
2	88.45	3397	38.41	3812	0.284
3	98.46	4197	42.63	4640	0.306
4	111.67	3474	31.11	4025	0.310
5	79.17	3664	46.29	4842	0.278
Mean	**97.91**	**3572**	**37.28**	**4592**	**0.361**
Std Dev	**14.35**	**399**	**7.68**	**724**	**0.149**
CV	**14.65**	**11.17**	**20.60**	**15.77**	**41.27**

Table 2.3: Mechanical properties of HNC

Hemp natural fibre composite-tensile – (HNC-TSL)					
Specimen	**Area (mm^2)**	**Peak load (N)**	**Peak stress (MPa)**	**Modulus of elasticity (MPa)**	**Poisson's ratio (mm/mm)**
1	180.35	5195	28.80	3026	0.409
2	190.51	5717	30.01	2820	0.367
3	166.28	5823	35.02	3356	0.403
4	183.82	6003	32.65	3081	0.383
5	188.08	5708	30.35	2959	0.391
Mean	**181.81**	**5689**	**31.37**	**3048**	**0.391**
Std Dev	**9.52**	**301**	**2.47**	**198**	**0.016**
CV	**5.24**	**5.29**	**7.87**	**6.50**	**4.09**

Source: Fajrin et al. (2013a)

Table 2.4: specimens' configuration for flexural test

Samples Code	**Skin**		**Intermediate layer**		**Core**		**Number of sample**
	Material	**Thickness**	**Material**	**Thickness**	**Material**	**Thickness**	
CTR	Aluminium	0.5 mm	None	-	EPS	21 mm	5
JFC	Aluminium	0.5 mm	Jute	3 mm	EPS	15 mm	5
HFC	Aluminium	0.5 mm	Hemp	3 mm	EPS	15 mm	5
						Total	15

Table 5.3. Experimental arrangements for flexural testing *(large scale)*

Samples Code	**Skin**		**Intermediate layer**		**Core**		**Number of sample**
	Material	**Thickness**	**Material**	**Thickness**	**Material**	**Thickness**	
CTR	Aluminium	1.0 mm	None	-	EPS	50 mm	5
JFC	Aluminium	1.0 mm	Jute	5 mm	EPS	40 mm	5
MDF	Aluminium	1.0 mm	MDF	5 mm	EPS	40 mm	5
						Total	15

Source: Fajrin et al. (2013a)

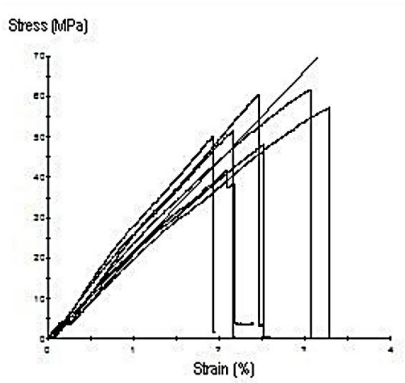

(a)

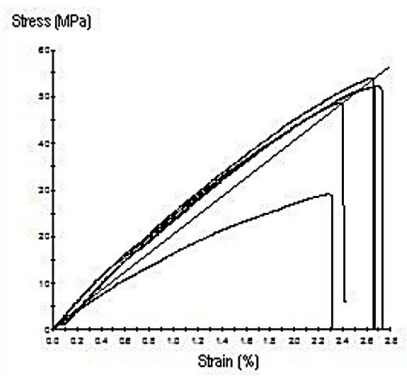

(b)

Source: Fajrin et al. (2013a)

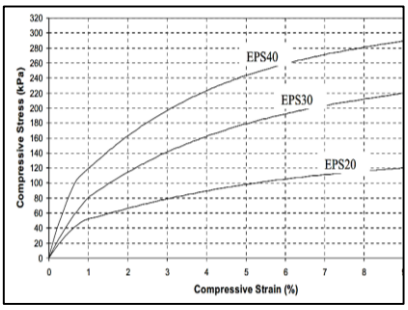

(c)

Source: Tewodros et al. (2010)

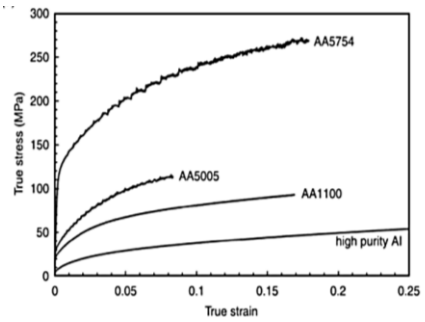

(d)

Source: (Lumley, 2011)

Figure 2.3: Stress-Strain curves for materials in this project:

(a) Jute Natural Fibre Composite

(b) Hemp Natural Fibre Composite

(c) EPS core

(d) Aluminium Skins

The boundary and loading conditions in the real experiment is shown in Figure 2.4 and a schematic of the four-point load applied in the test for medium and large specimens is illustrated in Figure 2.6 respectively. It is illustrated that the beam is under four-point bending load and simply supported by the apparatus supports.

Figure 2.4: Loading conditions in the real experiment

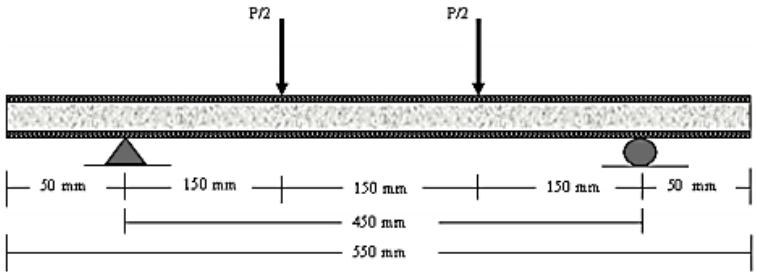

Figure 2.5: Schematic of four-point load for medium specimen

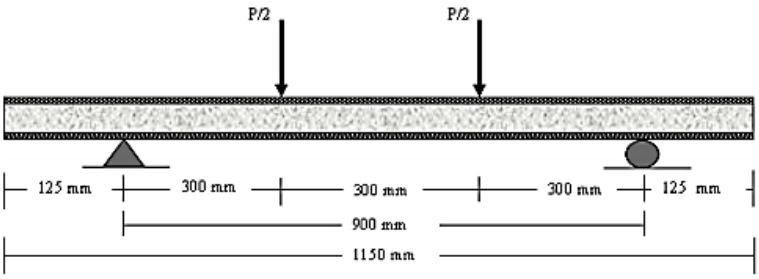

Figure 2.6: Schematic of four-point load for large specimen

Previous studies (Lanssens et al. 2014; Mousa & Uddin 2012) indicate that finite element modelling and analysis of SIPs has produced fairly accurate and reliable graphs. Figure 2.7 provides a good example of how close results obtained from finite element analysis (FE) could be to the data from the real experiment.

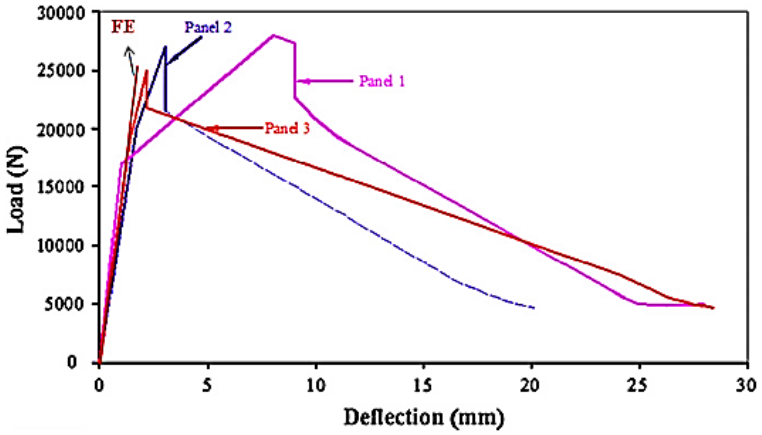

Figure 2.7: Load-deflection comparison between FEM and real experiment in previous studies

Source: (Mousa & Uddin 2012)

In Figure 2.7 , Panel 1, 2 and 3 are results of experiments in the laboratory and FE represents data generated by the finite element model

.

2.4.1 NFRP in construction industry

Increasing environmental concerns and global consciousness toward the natural resource preservation has attracted numerous researchers into the application of Natural fibre reinforced polymer (NFRP) in lieu of synthetic fibres in building industry as cost effective bio-composites. Natural fibres composite was first used in the construction of a primary school building out of jute fibre in Bangladesh in 1973 and followed by building house roofs and walls out of bagasse in Jamaica and Ghana and the Philippines in the 1980s. Moreover, the government of India supported jute based composite products as a wood alternative in building industry (Mathur 2006).

NFRP advantages are their low cost, high strength, low density, bio-degradability, environmentally friendly, non-corrosiveness and renewability. Natural fibres are available as coconut fibre (coir), jute, palm, hemp, abaca, sisal, bamboo, wood and paper in their natural condition (Herrera-Franco & Valadez-González 2004). Furthermore, (Burgueño, Quagliata, Mohanty, Mehta, Drzal &Misra 2004) stated that natural fibre biocomposites can improve the flexural strength of load-bearing components of a house. Moreover, (Dweib, Hu, O'Donnell, Shenton &Wool 2004) successfully utilised natural fibres to build a bio-based roof that meets the American standards of roof construction. Additionally, (Nasim & Rahul 2011) used NFRP laminate as face sheet and expanded polypropylene (EPS) as core to develop a new form of SIP known as natural structural insulated panel (NSIP). Their study shows that SIP conventional skin layers such as wood and glass fibre can be replaced by NFRP laminates.

Despite many studies report the benefits of using NFRP in the construction industry, more research needs to be done in order to reduce the cost of NFRP and expanding knowledge towards the structural behaviour of NFRP under loading.(Mohanty, Misra & Drzal 2005) argues that dimensional stability, specific strength and stiffness of single layered natural fibre based panels are far from desirable in the construction industry. Consequently, panels should be built in multiple layers which increase the overall cost.

3 Methodology

Major phases of the project from initiation towards completion are explained in this section. After installing Strand7 on the personal computer, it is important to have access to the manuals and tutorials that explain how 3D models can be built in Strand7. Also, it is crucial to be aware of how the experiment in the real world was conducted by Fajrin et al. (2013a). Details including experiment set up, load type, specimens dimensions, restraint conditions, material thickness and properties.

Main phases of the project are summarised as:

i) Research past papers and particularly, Fajrin et al. (2013a) in order to acquire in-depth knowledge of the experiment and test conditions
ii) Create medium and large 3D models of SIP and NFRP in strand7
   a. Model foam core using 3D brick element(Hexa8)
   b. Model top and bottom skin layers in SIP by 8 node isotropic rectangular bricks
   c. Model NFRP layer by 8 nodes isotropic bricks
   d. Use ‘extrude’ command to generate the foam core 3D mesh
   e. Insert the data for modulus of elasticity, tensile strength, density and elongation for aluminium, EPS and NFRP into Strand7. These values are shown in
   f. Table *2.1*,Table *2.2* andTable *2.3*.
   g. Apply support, boundary and load conditions to each specimen
   h. Run the model under various loads, NFRP layer type and thickness
iii) Record data in tables and plot the graph in Microsoft Excel
iv) Validate the results with experimental data
v) Discuss the influence of parameters in the study

4 Developing the 3D model

One of the major phases of this project was creating the nonlinear 3D model of the specimen based on the real experiment conducted by Fajrin et al. (2013a). Factors to be taken into account were global load, freedom cases, material properties, a graph of stress versus strain for each material, load factors and increments and checking load summation and warnings/errors at the end of the test. The initial step was to introduce the cross section of each specimen on XY plane and extrude the cross section in the Z axis.

The geometry of each specimen was taken from Fajrin et al (2013a) and entered into Strand7. It is important to set up units in Strand 7 at the beginning and stick to those units during the test. After setting up the software units, material properties were introduced to Strand7. All properties were taken from Fajrin et al. (2013a) as presented in section 2.4. As the specimens were going to be analysed non-linearly, the graph of stress versus strain for each material needed to be implemented in Strand7. Next step was to create nodes. Nodes represent the corner of each layer with specified thickness for that particular specimen. Then, materials were assigned to each group of nodes, boundary conditions were introduced and the load was applied.

As an example, for creating jute reinforced large scale specimen, jute, aluminium and EPS were introduced to Strand7 as ‘bricks’ as illustrated in Figure 4.1, Figure 4.2 and Figure 4.3 respectively.

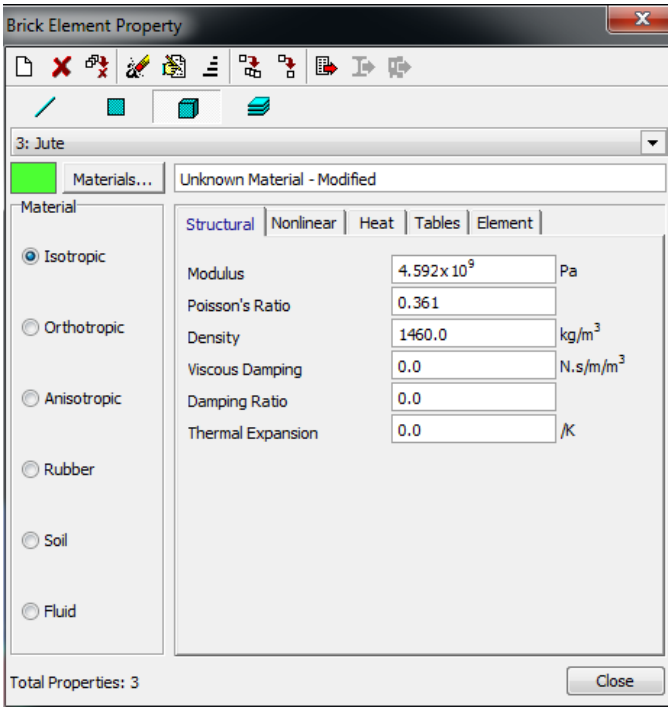

Figure 4.1: Properties of jute introduced to Strand7

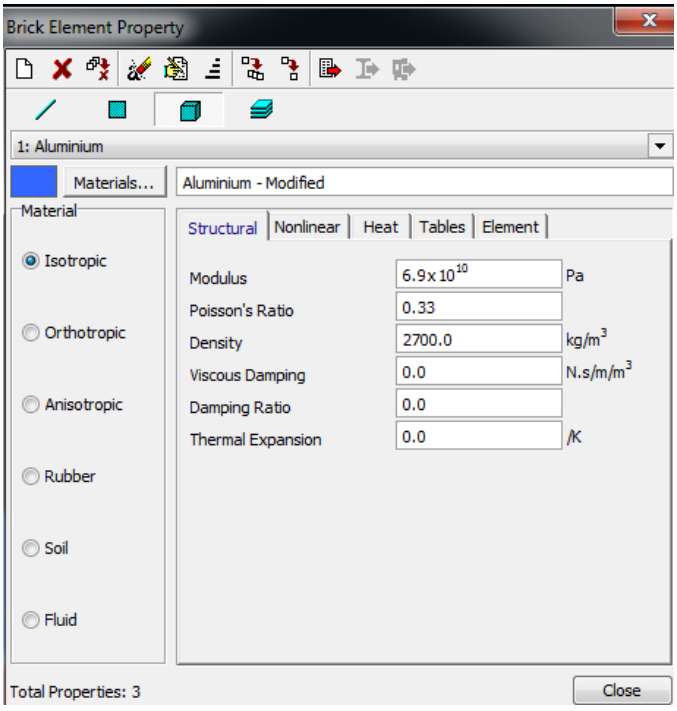

Figure 4.2:Properties of aluminium introduced to Strand7

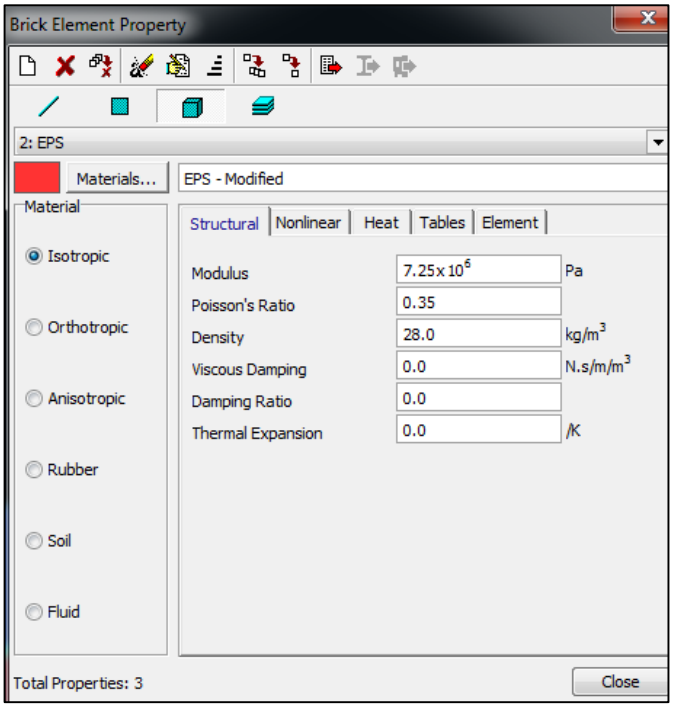

Figure 4.3: Properties of EPS core introduced to Strand7

Afterwards, in the non-linear section of each brick property, stress versus strain curve for each material was added based on Fajrin et al. (2013a). the graph of stress versus strain for all materials used in this project are shown in Figure 4.4Figure 4.5Figure 4.6Figure 4.7Figure 4.8.

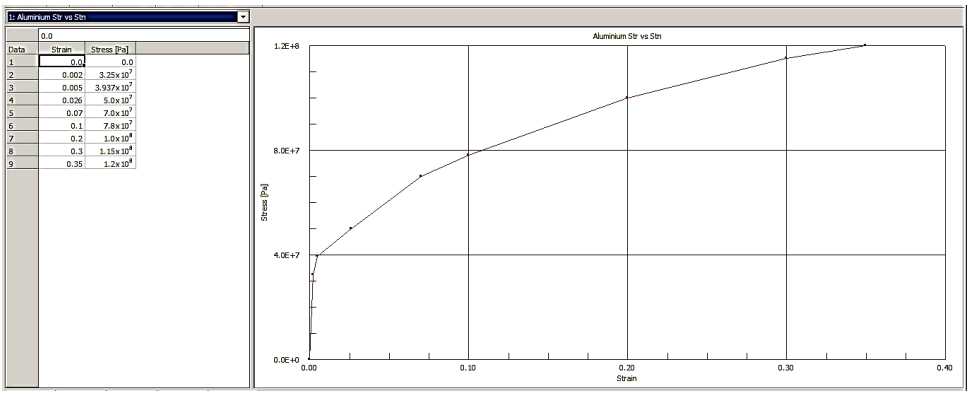

Figure 4.4: Graph of stress vs Strain for Aluminium

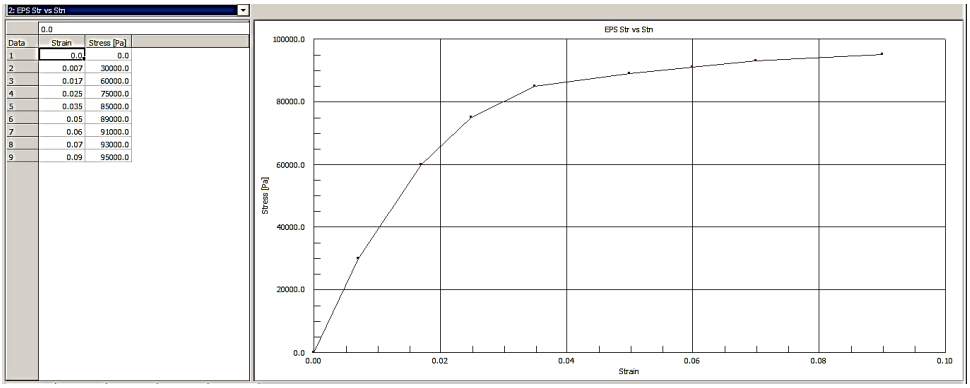

Figure 4.5:Graph of stress vs Strain for EPS Core

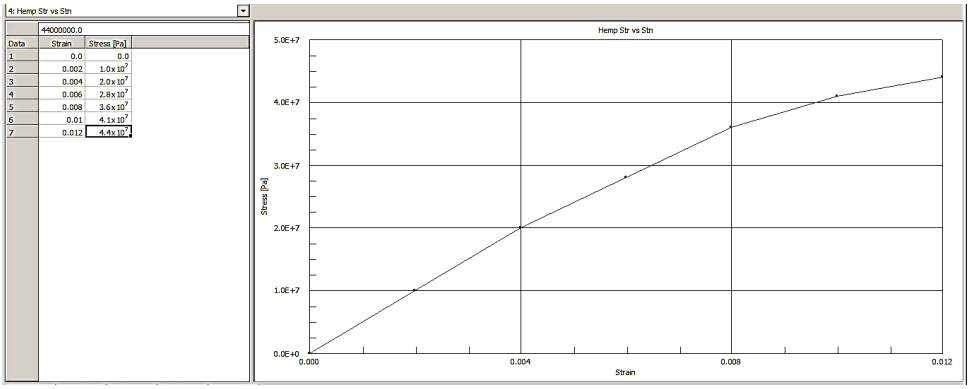

Figure 4.6: Graph of stress vs Strain for hemp

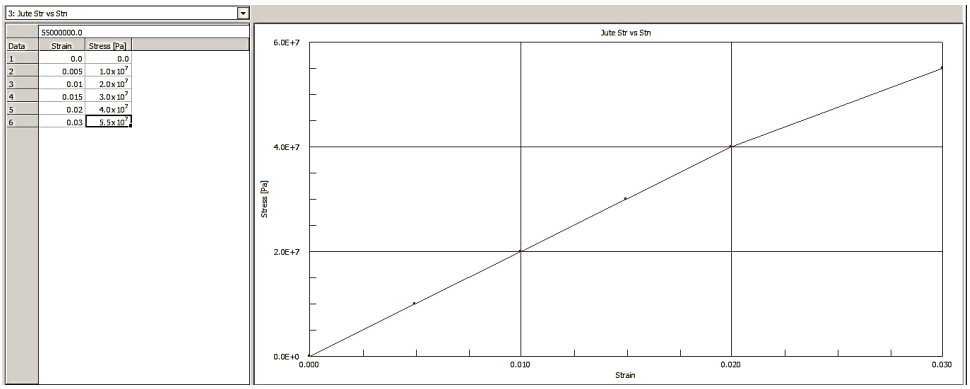

Figure 4.7: Graph of stress vs Strain for jute

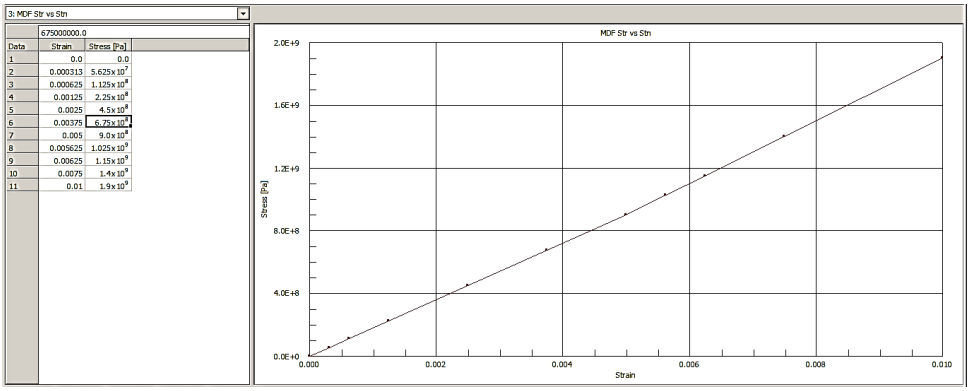

Figure 4.8: Graph of stress vs Strain for MDF

It is emphasised that the graph of stress versus strain could slightly change for each material as seen in Figure 2.3. This fact could be implemented when inserting the graph of stress versus strain for materials into Strand7. The next step after introducing materials was creating nodes. The coordinates of the first node, starting from the bottom, was introduced as (0, 0, 0). The second node; which is the width of the specimen; as (0.1, 0, 0) the third node; which represents the thickness of aluminium skin; as (0, 0.001, 0), the fourth node as (0.1, 0.001, 0). As such, the first skin layer of aluminium was created. To make the software understand that layers are connected to each other, the last two nodes of aluminium layer actually became the first two nodes of the jute fibre composite layer. By this, the next node which represents last two nodes of jute layer were entered as (0, 0.006,0) and next one as (0.1, 0.006,0) and henceforth for EPS and next layers of jute and aluminium in XY plane.

After creating the nodes, it was time to copy the nodes to achieve the span length (900 mm). this was done using ‘copy by increment’ command in ‘tools’. Then, using ‘Hexa 8’ command in ‘create element’ materials were assigned to nodes appropriately as shown in Figure 4.9. In this Figure, Aluminium is shown as blue, jute as green and EPS core as red. It was noticed that the order of the nodes is an important factor when connecting them to each other. Otherwise, the created element would not give desired results.

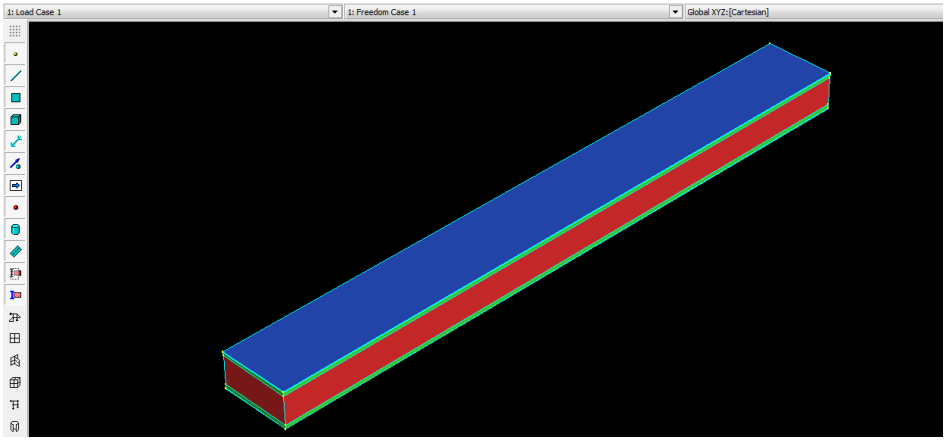

Figure 4.9: Initial steps of creating jute large scale specimen

The next step was to sub-divide the specimen to smaller cubes knows as elements in Strand7. More the elements are, more the time it takes for the software to analyse it and more accurate the result will be. Jute large specimen was subdivided into $48 \times 6 \times 5$ elements as shown in Figure 4.10.

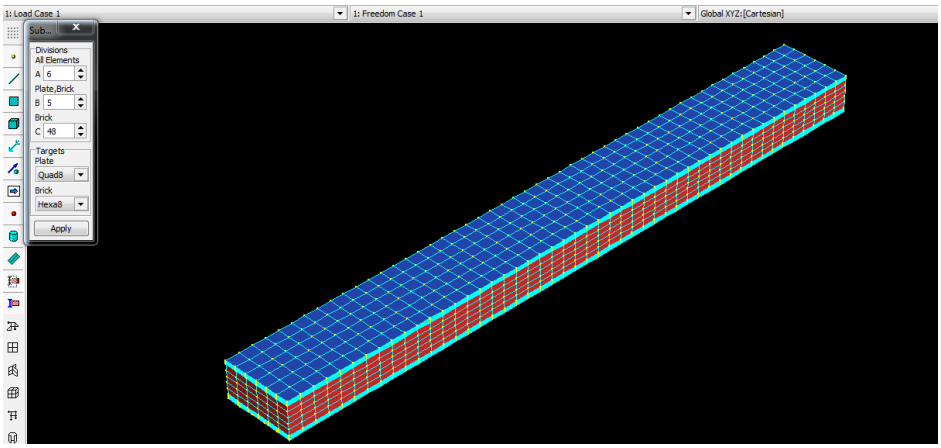

Figure 4.10: Subdividing jute large specimen

To best simulate the experimental conditions, one side was assigned as pin supported and the other side as roller support.

Applying load to the specimen needed special attention. As the test was being undertaken non-linearly, one Newton was divided by six and the result was applied to 1/3 and 2/3 of the span length as shown in Figure 4.11.

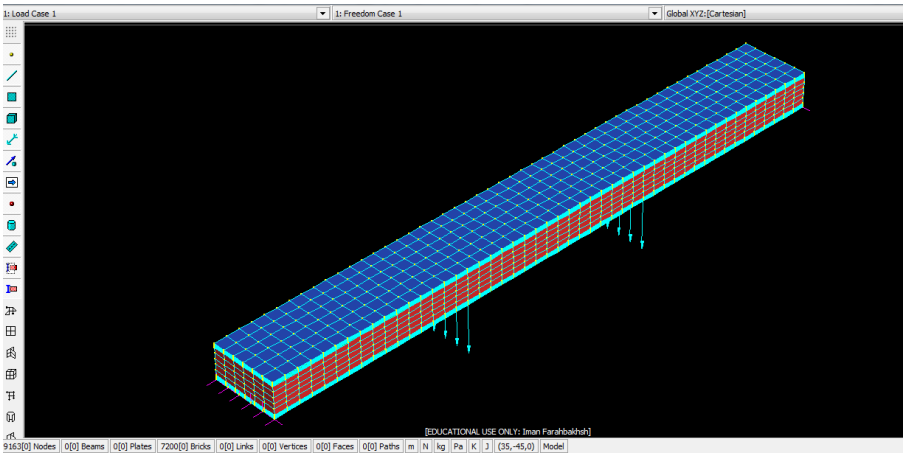

Figure 4.11: Load and boundary conditions applied to the specimen

For starting the analysis, 'non-linear static' was chosen in 'solver' command and 'load increments' were introduced based on the load-deflection graph from Fajrin et al. (2013a) as shown in Figure 4.12. For this project, 20 increments were chosen and the number of iterations was chosen automatically by Strand7 for convergence purposes. Load increments of all specimens are shown in Appendix E.

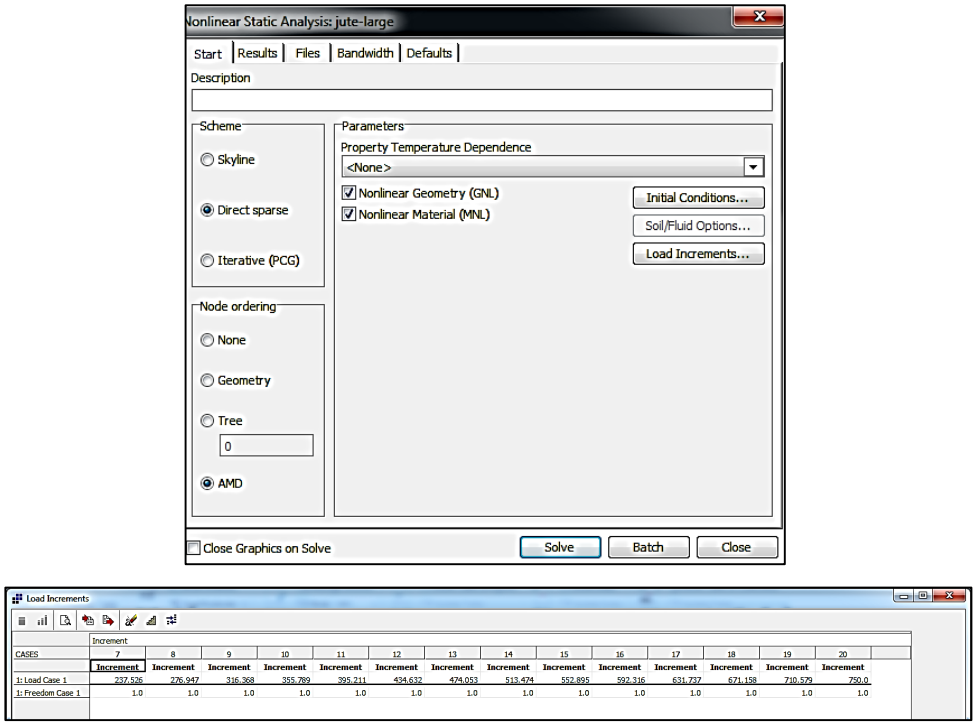

Figure 4.12: Non-linear static and load increments in Strand7

5 Results and discussion

In this section, results from the 3D model will be discussed and analysed. Also, these results will be compared against Fajrin et al. (2013a) for the validation purposes. Results will indicate whether the addition of an intermediate layer to SIPs will enhance the flexural properties of the panel or not. The graph of load versus deflection for each specimen was drawn and scaled into the experimental results in order to facilitate the comparison and validation purposes. Moreover, stress distribution in each sample was shown and discussed. It was noted that in the real experiment, the results were based on normalisation process in which the outliner data were not taken into account for calculation purposes.

It was found that in medium scale specimens, in average, adding an intermediate layer of jute and hemp fibre to the conventional sandwich panel will increase the load carrying capacity of the panel by 30% and 90% respectively. The 60% difference in the results indicated that hemp natural fibres have better performance under flexural loading in sandwich panels. It was also found that control specimen (without intermediate layer) and specimens with hemp intermediate layer had a higher level of stiffness than those with jute intermediate layer.

Results from large specimen analysis indicated that in average, load carrying capacity of the control specimen increased by 63% in specimens with jute intermediate layer and 170% in the specimen with MDF intermediate layer.

It was also found that addition of a natural fibre intermediate layer to the conventional sandwich panel decreased the maximum normal stress in the compression and tension layers of the specimen which enabled the specimen to carry more bending load compared to the specimen without an intermediate layer.

5.1 Comparison of load-deflection behaviour of specimens

Results acquired from Strand7 are illustrated and compared against results from the real experiment. It was found that in general, 3D models created by Strand7 were able to predict the behaviour of the control and hybrid

specimen with an acceptable level of accuracy. However, the ultimate failure load of the specimen was not achieved in this project due to delamination failure of the specimen in a real experiment. It will be discussed in more details in 'The recommendation for further work' chapter.

5.1.1 Medium specimens

The load-deflection graphs of medium scaled sandwich panels are shown in this section. It was seen that the behaviour of all samples followed a similar non-linear pattern which indicated the existence of a ductile material in the specimens. Resultant curves did not show any yield point, however, the load carrying capacity decreased sharply at the end of the plastic region which was a sign of initial failure. From this behaviour, it could be anticipated that the failure of the specimens would occur due to shear failure of the EPS core. The graphs illustrated a linear behaviour at the beginning which followed a non-linear pattern at the end.

In CTR samples as illustrated in Figure 5.1, it was seen that specimens showed a linear pattern until 105 N and 2.1 mm, then the graph initiated the non-linear portion until its final failure. As mentioned earlier, the final failure load was obtained from the real experiment and introduced to Strand7 models to stop the test in that load. Result for control specimen from Strand7 is shown as CRT-SP-ST7 and compared against results from the real experiment. As expected, the behaviour of the panel under bending load was dominantly controlled by the aluminium face sheets.

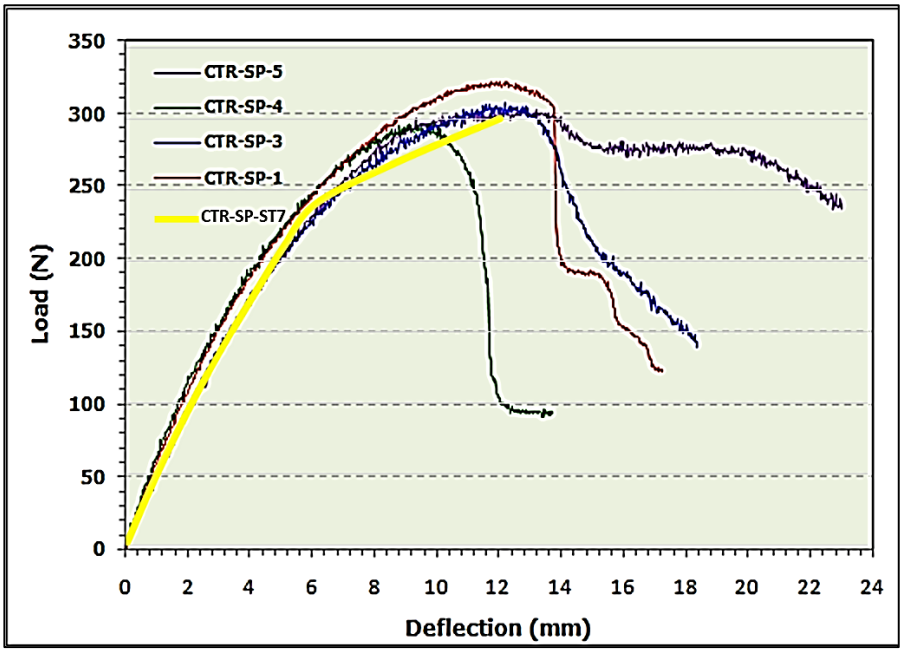

Figure 5.1: Comparison of results from Strand7 (ST7) with real experiment for medium scale control specimens

The load-deflection graph for medium scale specimens with jute intermediate layer is shown in Figure 5.2. JFC-SP specimen showed a uniform ductile behaviour same as the control specimen. The linear portion of the graph started from the origin and ended approximately at 145 kN with deflection of 10 mm. However, results from Strand7 was tending not to exactly follow the experiment results as shown in Figure 5.2. Ultimate load of 414 kN was found in the real experiment which was set as final load increment for Strand7 test for medium jute specimens. It was seen that in comparison with the control specimens, the average deflection of the jute specimens under the same load increased approximately three times. Fajrin et al. (2013) found that the delamination between core and jute intermediate was a major cause of failure in jute specimens however, it was out of the scope of this project. As expected for typical ductile material, no yield point was observed in the graph of load versus deflection for jute specimens.

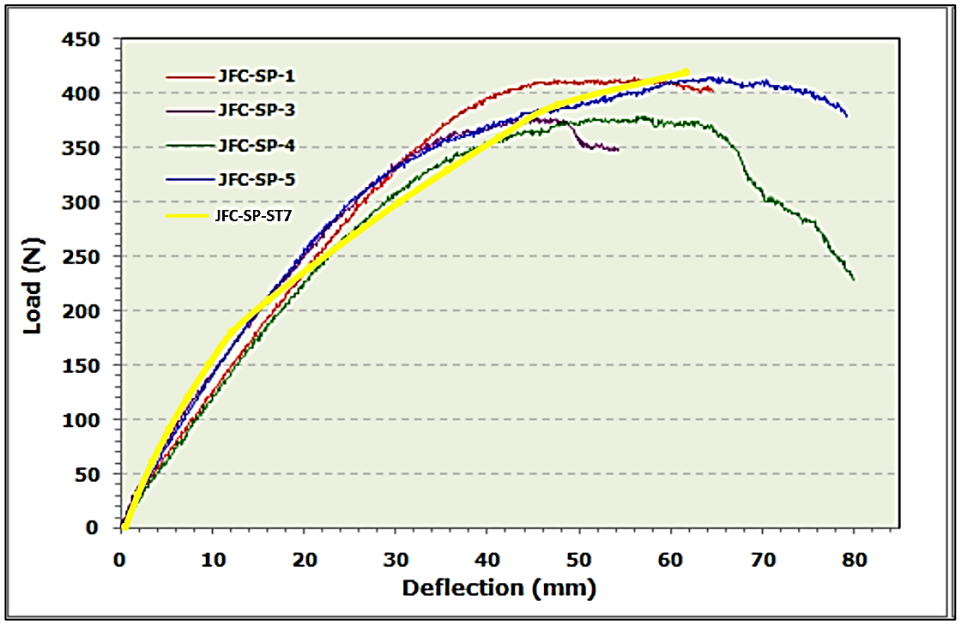

Figure 5.2: Comparison of results from Strand7 (ST7) with real experiment for medium-scaled specimens with jute intermediate layer

The load versus deflection for sandwich panels with hemp fibre intermediate layer (HFC-SP) is shown in Figure 5.3. in the real experiment, hemp specimens showed a substantial variation in their results. However, results from Strand7 showed an acceptable deflection range over the applied load compared with the real experiment. In HFC specimen, the overall behaviour of HFC specimens also followed a typical ductile material with no yield point. As seen in Figure 5.3, in real experiments, there has been an abrupt drop in load carrying capacity when the applied load reaches around 600 N which was not observed in results obtained from Strand7. However, computer simulation results can be used to predict the overall behaviour of HFC specimen until the failure point.

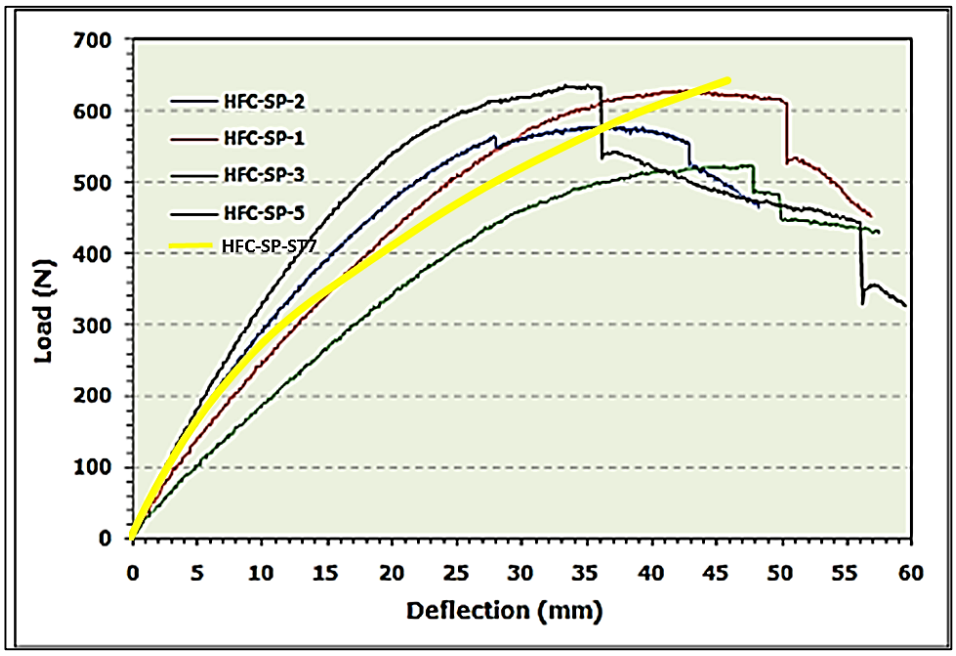

Figure 5.3:Comparison of results from Strand7 (ST7) with real experiment for medium-scaled specimens with hemp intermediate layer

For comparison purposes, results obtain from Srand7 for medium scale specimen with no intermediate level, specimen with jute intermediate layer and specimen with hemp intermediate layer were plotted on the same graph as Figure 5.4. It was seen that the introduction of an intermediate layer of jute and hemp significantly increased the load carrying capacity of the sandwich panel. It was also observed that addition of an intermediate layer of jute and hemp increased the ductility of the composite panel compare to the conventional panel. In terms of the stiffness of the specimen, it was realised that specimen with jute intermediate layer showed less stiffness compared to control and HFC specimen.

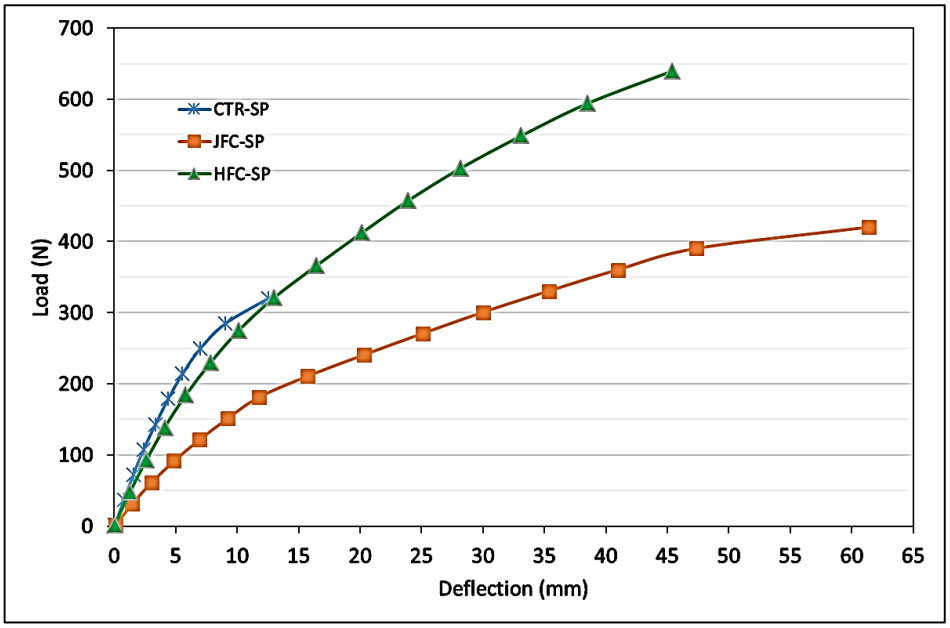

Figure 5.4: comparison of load carrying capacity among medium scale specimens

5.1.2 Large specimens

The load-deflection graphs for large specimens are presented in this section. Figure 5.5 shows the load-deflection graph for large scale control specimen with no intermediate layer. The overall pattern was seen to be similar to the conventional medium scale specimens. The linear portion started from the origin and continued until 295 N, followed by a non-linear part until the ultimate load. Similar to the medium scale specimen, the ultimate load was introduced to the models in this project in which Strand7 stopped the test. The load carrying capacity of the specimen decreased gradually near the failure load. The specimen showed a stiffening behaviour during the test. Again there was no yielding point observed in the obtained result as commonly observed for a ductile material. The deviation of the graph was clearly observed after the linear portion until reaching the failure load. Overall, the load-deflection graph of large scale specimen with no intermediate layer followed an anticipated pattern similar to the medium scale specimen.

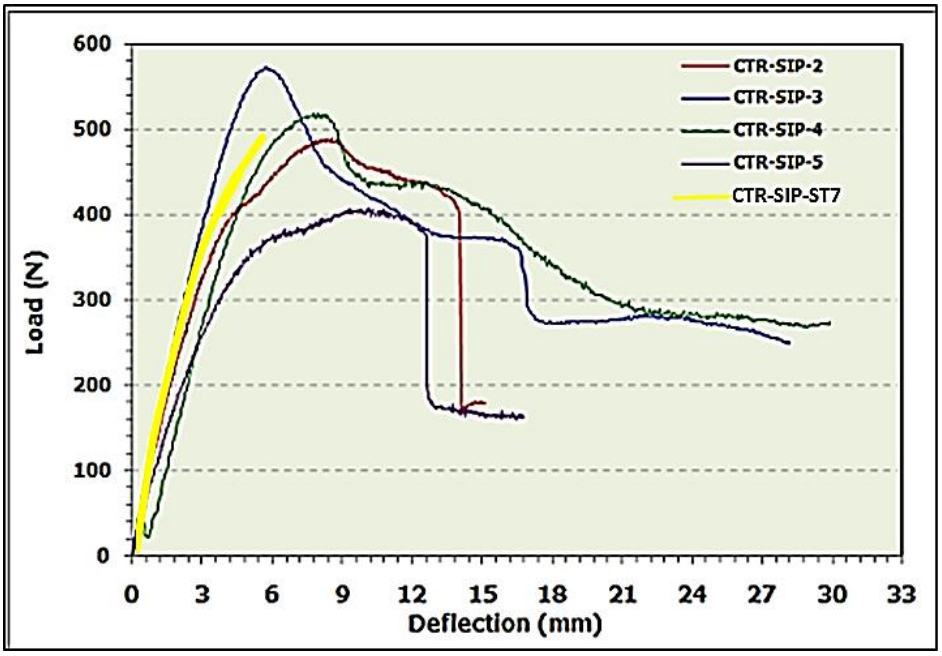

Figure 5.5:Comparison of results from Strand7 (ST7) with real experiment for large scale control specimens

Figure 5.6 shows the load-deflection behaviour of large scale specimen with jute intermediate layer. The graph started with a straight line from the origin and continued to approximately 198 N and then, started to gradually deviate into the plastic region until the ultimate load near 800 N. The graph steadily moved away the linear part and no yielding point was observed. Maximum deflection for JFC-SIP specimen was observed to be 39 mm at an applied load of 805 N.

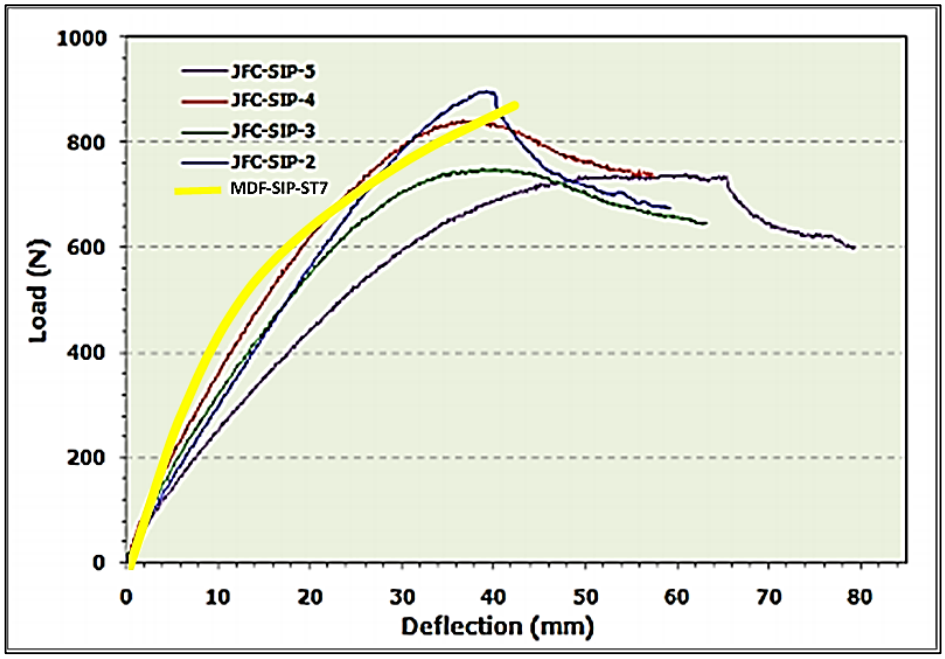

Figure 5.6:Comparison of results from Strand7 (ST7) with real experiment for large-scaled specimens with jute intermediate layer

The load-deflection graph of sandwich panels with MDF intermediate layer is shown in Figure 5.7. It was seen that MDF-SIP specimens behaved like a typical ductile material. The initial linear portion started from the origin, continued to approximately 600 N and then deviated into the non-linear part forming a plastic region. Same as other specimens, no yielding point was seen for these specimens. A higher level of relative stiffness with smaller deflection was observed in results from the specimen with MDF intermediate layer compared with all other specimens in this report. Also, higher load carrying capacity and steady behaviour.

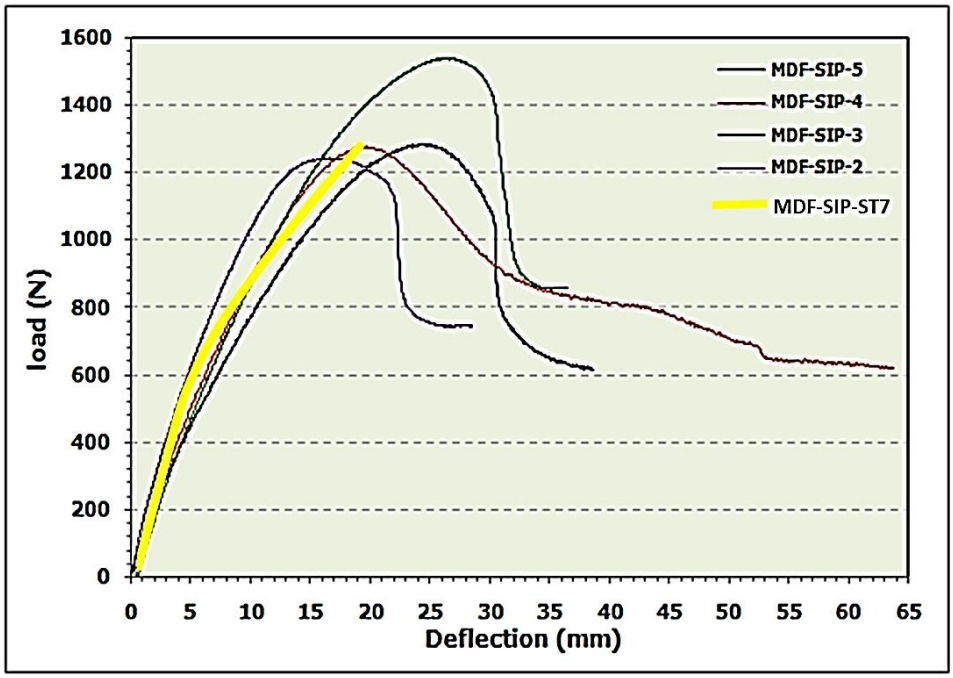

Figure 5.7:Comparison of results from Strand7 (ST7) with real experiment for large scale specimens with MDF intermediate layer

The comparison of the results from large scale specimens with no intermediate layer (CTR-SIP), jute intermediate layer (JFC-SIP) and MDF intermediate layer (MDF-SIP) is shown in Figure 5.8. It is clearly seen that the addition of intermediate layers of jute and MDF significantly increased the load-carrying capacity of the conventional insulated panels. Sandwich panels with MDF intermediate layers were much stiffer than those with the jute fibre intermediate layer. Also, in terms of load carrying capacity, MDF-SIP was the winner with an average of 1300 N and 20 mm of deflection. This means an increase of 170% in load carrying capacity compared to the conventional sandwich panels. At a similar load of 450 N, the deflection in CTR specimens reached 5.5 mm while in JFC-SIP, the deflection was nearly double that amount for the same applied load. MDF-SIP specimen showed a deflection of 4 mm in the same exerted load.

All specimen showed ductile behaviour to a certain level. Specimen with jute intermediate layer showed less stiff behaviour, however, their high level

of ductility, compared to CTR-SIP and MDF-SIP specimens, makes them suitable to be utilised in the building industry.

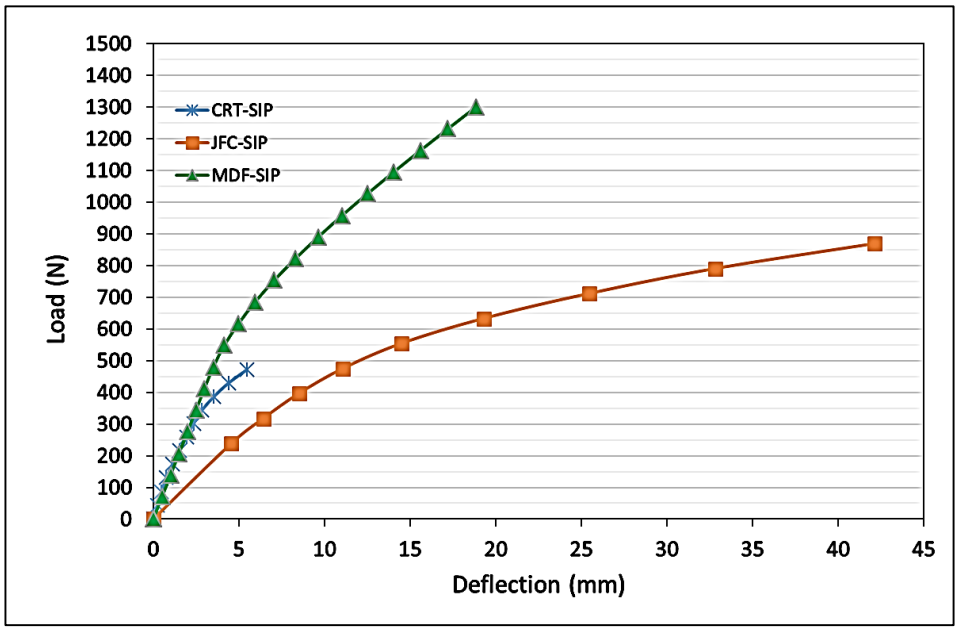

Figure 5.8:comparison of load carrying capacity among large scale specimens

Toughness is the ability of a material to resist the applied load even after cracks appear in the material. Toughness of a material can be measured by the area under the load-deflection curve of that material. Sandwich panels with intermediate layer showed much larger area under their load-deflation graphs which represent a higher value of their toughness. In terms of toughness values, JFC-SIP specimens showed larger toughness values compared to two other specimens which means it will require more amount of energy to produce a specific amount of damage to these specimens. This quality makes them stand out of the other specimens for building purposes.

However, it is not only the toughness that shall be considered in choosing a material for building. Somayaji (1995) argues that stiffness and strength are the most important factors to be considered when choosing a building material. stiffness and strength of a material describe the amount of material's deflection under specific load and the relative load magnitude that

the material is able to take before failure. These characteristics relate to the elastic range of the load-deflection graph and stress-strain graph. Relatively large deflection of sandwich panels is another important factor to be considered when choosing a material for building purposes.

5.2 Comparison of theoretical and 3D model deflections

Formulae for calculating the theoretical deflection of sandwich panels under bending was introduced and discussed in section 2.2. In this section, estimated theoretical values are compared with the computer generated deflection values acquired from Strand7 models. Two loads of 50 N and 100 N were chosen for comparison purposes. A sample calculation is shown in Appendix B. For most specimens, theoretical deflection values were larger than the computer generated values. The difference between theoretical and computer generated models ranged from 2.1% to 31.1%. The summary of data is shown in Table 5.1.

Table 5.1: Comparison of the theoretical deflections with Strand7 3D models deflections

sample	b	tc	$(EI)_{eq}$	p	δ_{theo}	δ_{ST7}	$\delta_{theo} - \delta_{ST7}$	% difference
CTR-SP	50	21	478993112	50	1.25	1.06	0.19	15.2
CTR-SP	50	21	478993112	100	2.62	2.1	0.52	19.8
JFC-SP	50	15	509155411	50	2.12	1.98	0.14	6.6
JFC-SP	50	15	509155411	100	4.22	4.31	-0.09	-2.1
HFC-SP	50	15	546612604	50	1.79	1.62	0.17	9.5
HFC-SP	50	15	546612604	100	3.55	3.42	0.13	3.7
CTR-SIP	100	50	9666786823	50	0.58	0.56	0.02	3.4
CTR-SIP	100	50	9666786823	100	1.19	0.97	0.22	18.5
JFC-SIP	100	40	1.137E+10	50	0.79	0.76	0.03	3.8
JFC-SIP	100	40	1.137E+10	100	1.51	1.98	-0.47	-31.1
MDF-SIP	100	40	9908906111	50	0.76	0.71	0.05	6.6
MDF-SIP	100	40	9908906111	100	1.58	1.52	0.06	3.8

It was seen that for control specimens, the difference between theoretical and 3D models deflections ranged from 15% to 19%. For specimens with jute intermediate layer, this value varied between 2.1% to 31%, for specimens with hemp intermediate layer, the range was from 3.7% to 9.5% and for samples with MDF intermediate layer, it varied from 3.8% to 6.6%. It was expected that with increasing bending stiffness in specimens,

deflection decreases. However, it was seen that this theory could be not always true. In JFC specimens, the deflection of the panel was much higher than those without any intermediate layer under the same load.

Medium specimens with jute and hemp intermediate layer had the theoretical deflection value of 2.12 and 1.79 mm under 50 N of applied load. While, control specimen had the theoretical value of 1.25 mm. It was due to the bending and shear deformation of the core that contributed to the overall deflection of the panel. It was understood that the overall bending deflection would have had smaller values without shear deflection of the core. This finding was confirmed by Sharaf et al (2010) that stated that the shear deformation was a major contributor to the overall deflection of sandwich panels with low-density cores under bending. They stated that about 75% of the overall deflection of sandwich panels was caused by shear deformation of the soft core. However, they reported this fraction to be about 50% for sandwich panels with a hard core.

Considering the significance of the shear deformation in sandwich panels with a soft core, the geometric characteristics of the specimen including the width and the core thickness, are of crucial factors in the value of the overall deflection. Control specimen, have a larger core thickness compared to specimens with jute and hemp intermediate layers. It can be seen that the overall deflection of CTR panels is less than those counterparts.

In the large scale specimens, similar to medium scale ones, the theoretical deflection of the panel was in a reasonable agreement with the deflections obtained in 3D models. It was seen that the deflection values from the 3D models were lower than the theoretical values. For the control specimens, the difference between the Strand7 results and theoretical deflection values ranged from 3.4% to 18.5%. This value was between 3.8% to 31.1% for specimens with jute intermediate level and 3.8% to 6.6% for specimens with MDF intermediate layer. It was noticed that the contribution of the shear deformation in overall deflection of the specimens was remarkable having a range between 86% to 94% of the overall deflection. This meant that the contribution of the bending deflection was between 6% to 14%. A higher

value of bending stiffness was observed in the specimens with intermediate layer however, larger deflections were seen due to thinner core. Therefore, it can be argued that the introduction of intermediate layer did not result in reduction in the deflection of the specimens as the main contributor to the overall deflection of the panels was the shear deformation of the core.

5.3 Normal stress distributions of specimens

Due to bending forces, tension and compression occurred along the longitudinal line of the specimens (Z axis in this study). Normal stress distribution for all specimens are presented and analysed in this section. It is stated that shear stress distribution of specimens is illustrated in Appendix D. Figure 5.9 shows the normal stress distribution in medium scale control specimen. As expected, maximum stress occurred in compression (maximum negative) and tension (maximum positive) plains, taken by the aluminium skins. The maximum negative stress in medium scale control specimen was -40.5 MPa and the maximum positive stress in tension layer was 41.5 MPa. These numbers are important for comparison purposes with medium scaled specimens with jute and hemp intermediate layers.

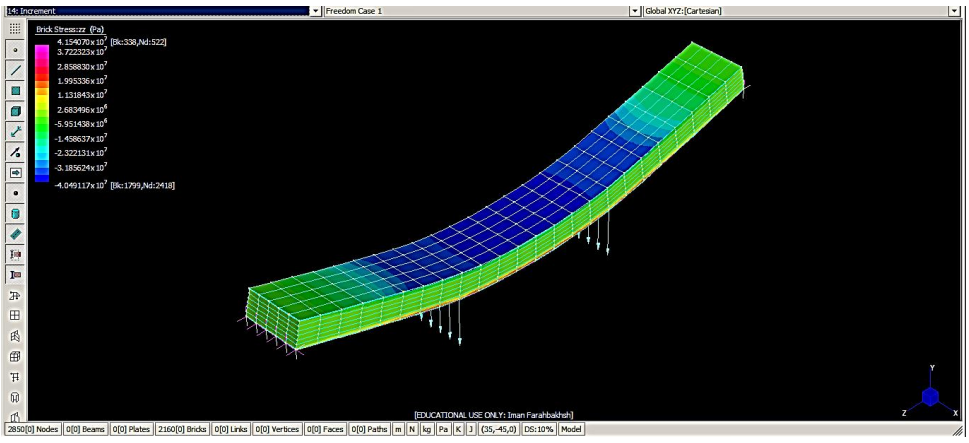

Figure 5.9: Normal stress distribution in CTR-SP

Normal stress distribution of JFC-SP is illustrated in Figure 5.10. Similar to the control specimen, the maximum compressing stress was taken by the aluminium face on top and the largest tensile stress occurred on the lowest layer in the aluminium face sheet. However, the magnitude of the maximum negative normal stress reduced to -27.1 MPa and the largest amount of positive normal stress to 24.8 MPa. It means that the addition of jute intermediate layer resulted in 40.2% reduction in the extreme normal stress in the panel. Jute natural fibre was responsible for taking a relatively large amount of stress as shown in light blue areas in the picture. The magnitude of stress in the intermediate layer was seen to be approximately between 11 to 16 MPa which equalled to 52% of the maximum normal stress in the panel. Taking this amount of stress in the panel resulted in a high amount of toughness in JFC-SP as discussed in section 5.1.

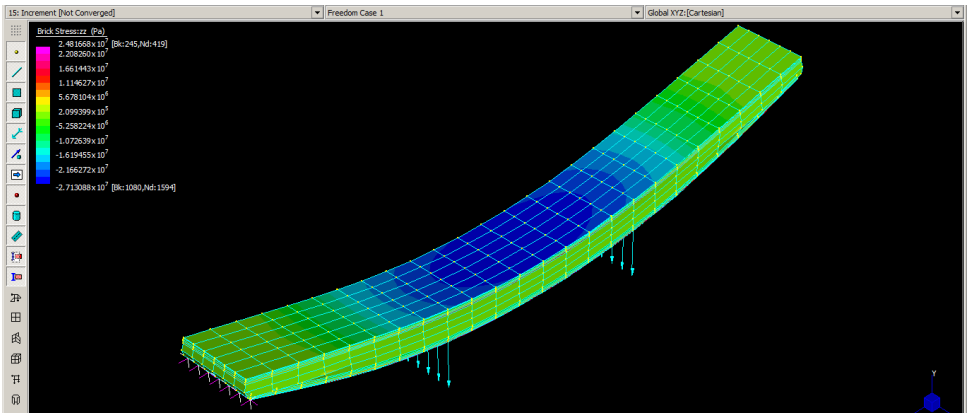

Figure 5.10: Normal stress distribution in JFC-SP

Figure 5.11 shows normal stress distribution in specimen with hemp intermediate layer. The maximum negative stress taken by the panel was -26.7 MPa and the maximum positive normal stress appeared to be 25.4 MPa. These numbers were close to maximum normal stress in the specimen with jute intermediate layer. The extreme normal stress in HFC-SP specimen was seen to be 38.7% less than the same category in control specimens. This reduction resulted in an increase in load carrying capacity by the specimen compared to the control specimen. Stress taken by hemp

intermediate layer ranged between 10.5 to 15 MPa which was close to the range of its counterpart, jute natural fibre.

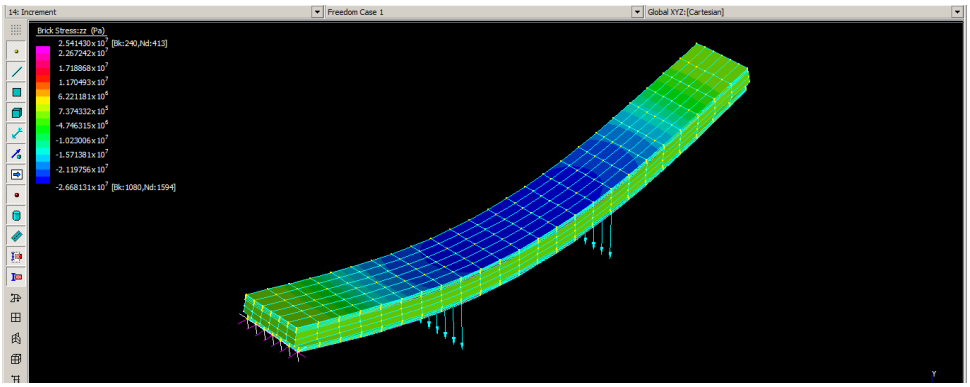

Figure 5.11: Normal stress distribution in HFC-SP

For large scale specimens, the distribution of normal stress was seen to be slightly different to the medium scale specimens. As shown in Figure 5.12 , in large scale control specimens, negative normal stress was maximum in the top aluminium skin, close to the location of the vertical load exertion. However, light blue colour on the top surface of the panel, seen in the picture, confirmed that the largest amount of stress was taken by the aluminium face sheets with the magnitude of -52 MPa. The largest amount of positive stress was taken by the aluminium skin at the bottom face of the panel with the magnitude of 66.7 MPa. Compared to the medium scale control specimen, the amount of stress in the compression and tension layers increased by 37.8%. Moreover, the behaviour of the panel under bending load was required to be studied in further detail. The nice curve shape of the control specimen in medium scale specimen changed to a semi-broken shape with more visible angles that clearly showed the location of the load application. It could be due to the shear stress distribution of the core under a higher amount of bending load. Furthermore, it was noticed that the size of the large control specimen got doubled compared to the medium control specimen however, the amount of normal stress in this specimen increased by 37.8%. Therefore, it could be understood that increasing the size of a

specimen by a specific amount will not necessarily increase the normal stress by that amount in sandwich panels.

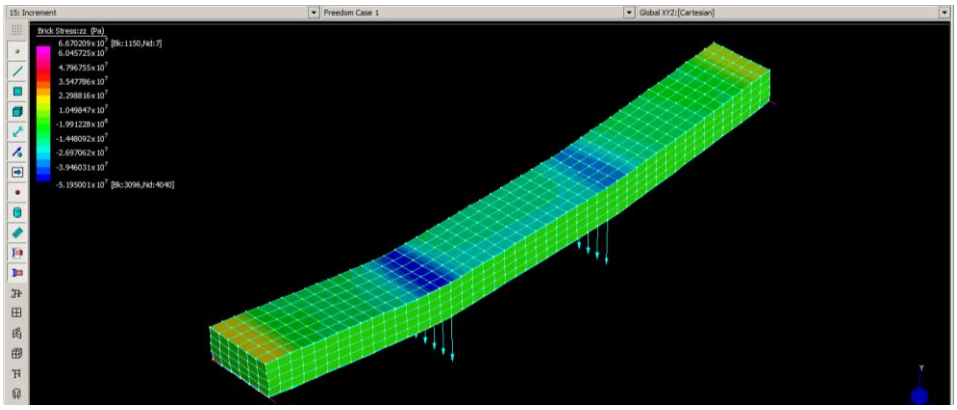

Figure 5.12: Normal stress distribution in CTR-SIP

Normal stress distribution in large scale specimen with jute intermediate layer, shown in Figure 5.13, indicated a similar pattern to medium scale specimens with the largest negative stress on the top layer and the maximum positive stress in the most bottom layer of the panel. The maximum negative normal stress was -51.1 MPa and the maximum positive normal stress was 56.2 MPa. The reduction in the maximum normal stress in the panel was seen to be 15.7% compared to the large control specimen. This amount was 24.5% less than the stress reduction in JFC-SP. The range of normal stress in large scale jute natural fibre layer was between 17.2 MPa to 29.5 MPa in both compression and tension layers of the panel. This amount equalled to 47.5% of the maximum stress in JFC-SIP which was 4.5% less than the normal stress in jute intermediate layer in JFC-SP. This could relate to the lower amount of reduction in the maximum normal stress in the hybrid panel.

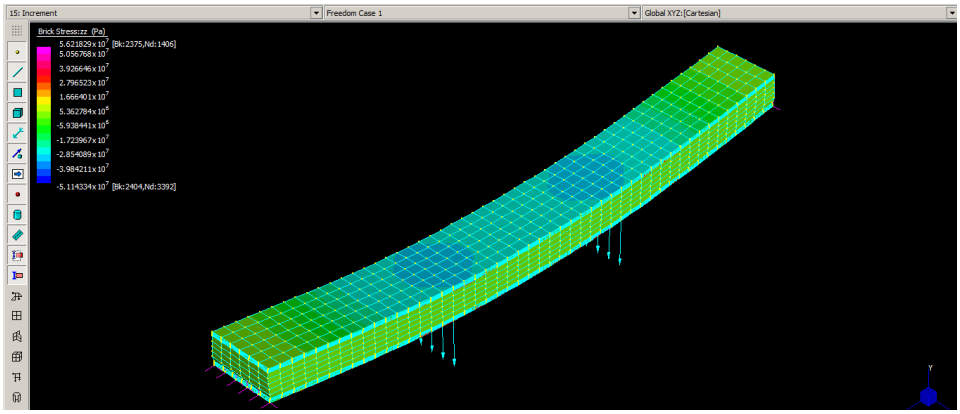

Figure 5.13: Normal stress distribution in JFC-SIP

Normal stress distribution in MDF-SIP specimen is shown in Figure 5.14. It was seen that maximum negative stress occurred at the compression layer with a magnitude of -15.8 MPa and the maximum positive stress was 18.24 MPa in the tension layer of the specimen. Compared to the control specimen, the maximum normal stress in the panel reduced by 72.7%. This significant reduction in the magnitude of the maximum stress confirmed the remarkable positive effect of using a natural intermediate layer in conventional structural panels. The largest stress reduction among all specimens of this study occurred in MDF-SIP. This could verify the largest amount of load carrying capacity observed in specimens in section 5.1. Stress distribution in MDF intermediate layer ranged between 5 to 8.5 MPa; the smallest among all other intermediate layers. This could make MDF-SIP a highly favourable material to be utilised in the building industry.

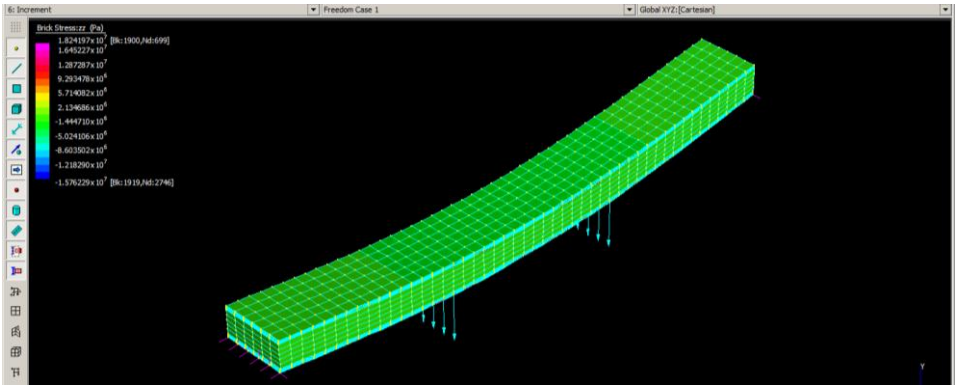

Figure 5.14: Normal stress distribution in MDF-SIP

6 Conclusion and recommendations

In this project, Strand7 was used to create 3D models to study the effect of adding natural fibre intermediate layers to the conventional sandwich panels. The real experiment of this study had been undertaken at the University of Southern Queensland and results from that study were used o validate the results from Strand7 models. Overall results from Strand7 showed a high level of accuracy against the real experiment results. It was found that adding an intermediate layer of natural fibres could increase the load carrying capacity of the conventional structural panels up to 170% and decrease the maximum normal stress in the panel by 72.7%. Specimens with jute intermediate layer showed a lower amount of stiffness compared to specimens with hemp and MDF intermediate layer.

Results from this study showed that sandwich panels reinforced with natural fibre layers can be a highly advantageous to be used in the construction and building industry. Biodegradability, non-corrosive characteristics and vast availability of natural fibres make them suitable materials for building industry. They can reduce the cost of the sandwich panels by reducing the required thickness of the aluminium face sheets and at the same time, increase the load carrying capacity of the conventional panels.

7 Recommendations for further work

Due to time constraints and complexity of the topic, the bonding agent in specimens were not modelled in this project. Hence, the final failure loads of the specimens were not achieved. It is recommended for further research to model the adhesive that bonds the layers together in order to predict the failure point of each specimen. To do so, it is recommended to create a uniform thin layer of the adhesive in the shape of a layer and test it to obtain the mechanical properties as well as the graph of stress versus strain of the adhesive. Acquired properties can be inserted into Strand7 models to predict the failure point of the specimens.

8 References

Abang Abdullah Abang, A, Mohammad, P & Yen Lei, V 2013, 'Structural Insulated Panels: Past, Present, and Future', *Journal of Engineering*, vol. 3, no. 1, pp. 2-8.

Anon, 2016. *Stresses: Beams in Bending*. 1st ed.

ASTM Standard C 393 (2000), *Standard test method for flexural properties of sandwich construction*, ASTM C393-00, ASTM International, Philadelphia, Pa 19103.

Burgueño, R., Quagliata, M., Mohanty, A., Mehta, G., Drzal, L. and Misra, M., 2004. Load-bearing natural fiber composite cellular beams and panels. *Composites Part A: Applied Science and Manufacturing*, 35(6), pp.645-656.

Davies, J., 2001. *Lightweight sandwich construction*. Oxford: Blackwell Science.

Dweib, MA, Hu, B, O'Donnell, A, Shenton, HW & Wool, RP 2004, 'All natural composite sandwich beams for structural applications', *Composite Structures*, vol. 63, no. 2, pp. 147-157.

Fajrin, J, Zhuge, Y, Bullen, F & Wang, H 2013a, "Hybrid sandwich panel with natural fibre composite intermediate layer: Manufacturing process and significance analysis".

Fajrin, J, Zhuge, Y, Bullen, F & Wang, H 2013b, "Significance analysis of flexural behaviour of hybrid sandwich panels".

Gnip, IJ, Vaitkus, SI, Kersulis, VI & Veyelis, SA 2007, 'Deformability of expanded polystyrene under short-term compression', *Mechanics of Composite Materials*, vol. 43, no. 5, pp. 433-444.

Herrera-Franco, PJ & Valadez-González, A 2004, 'Mechanical properties of continuous natural fibre-reinforced polymer composites', *Composites Part A*, vol. 35, no. 3, pp. 339-345.

Hibbeler, R., 1997. *Mechanics of materials*. Upper Saddle River, N.J.: Prentice Hall.

Hidallana-Gamage, HD, Thambiratnam, DP & Perera, NJ 2014, 'Numerical modelling and analysis of the blast performance of laminated glass panels and the influence of material parameters', *Engineering Failure Analysis*, vol. 45, pp. 65-84.

Ku, H, Wang, H, Pattarachaiyakoop, N & Trada, M 2011, 'A review on the tensile properties of natural fiber reinforced polymer composites', *Composites Part B*, vol. 42, no. 4, pp. 856-873.

Lanssens, T, Tanghe, C, Rahbar, N, Okumus, P, Van Dessel, S & El-Korchi, T 2014, 'Mechanical behavior of a glass fiber-reinforced polymer sandwich panel with through-thickness fiber insertions', *Construction and Building Materials*, vol. 64, pp. 473-479.

Lumley, R., 2011. *Fundamentals of aluminium metallurgy*. Oxford: Woodhead Pub.

Mamalis, AG, Spentzas, KN, Manolakos, DE, Pantelelis, N & Ioannidis, M 2008, 'Structural and impact behaviour of an innovative low-cost sandwich panel', *International Journal of Crashworthiness*, vol. 13, no. 3, pp. 231-236.

Manalo A., Aravinthan T., Karunasena W., Islam M.M., (2009), Flexural behavior of structural fiber composite sandwich beams in flatwise and

edgewise positions, *Composite Structures*; doi:10.1016/j.compstruct.2009.09.046.

Mathur, VK 2006, 'Composite materials from local resources', Construction and Building Materials, vol. 20, no. 7, pp. 470-477.

Mohanty, AK, Misra, M & Drzal, LT 2005, Natural fibers, *biopolymers, and biocomposites*, Taylor & Francis, Boca Raton, FL.

Mostafa, A., Shankar, K., Morozov, E.V. 2013, 'Effect of shear keys diameter on the shear performance of composite sandwich panel with PVC and PU foam core: FE study', *Composite Structures*, vol. 102, pp. 90-100.

Mousa, MA & Uddin, N 2012, 'Structural behavior and modeling of full-scale composite structural insulated wall panels', *Engineering Structures*, vol. 41, pp. 320-334.

Nasim, U & Rahul, RK 2011, 'Manufacturing and Structural Feasibility of Natural Fiber Reinforced Polymeric Structural Insulated Panels for Panelized Construction', *International Journal of Polymer Science*, vol. 2011.

Ramroth, WT, Asaro, RJ, Zhu, B & Krysl, P 2006, 'Finite element modelling of fire degraded FRP composite panels using a rate dependent constitutive model', *Composites Part A*: Applied Science and Manufacturing, vol. 37, no. 7, pp. 1015-1023.

Roylance D., 2000, *Beam Displacements*, Department of Materials Science and Engineering, Massachusetts Institute of Technology, Cambridge, USA.

Sharaf T., Shawkat W., Fam A., 2010, Structural performance of sandwich wall panels with different foam core densities in-one-way bending, *Journal of Composite Materials,* Vol. 44, No 19, 2010.

Somayaji S., 1995, *Civil engineering materials,* Prentice Hall, Englewood, New Jersey, USA.

Steeves, CA & Fleck, NA 2004, 'Collapse mechanisms of sandwich beams with composite faces and a foam core, loaded in three-point bending. Part II: experimental investigation and numerical modelling', *International Journal of Mechanical Sciences,* vol. 46, no. 4, pp. 585-608.

Tewodros H. Tefera, Roald A, Hermann B, Kristian A, 2010, ' FEM simulation of full scale and laboratory models test of EPS', *The Norwegian Public Roads Administration*, Norway.

Tornabene, F, Brischetto, S, Fantuzzi, N & Viola, E 2015, 'Numerical and exact models for free vibration analysis of cylindrical and spherical shell panels', *Composites Part B: Engineering,* vol. 81, pp. 231-250.

Zenkert, D. 1995, *AN introduction to sandwich construction*, Solihull, EMAS.

Appendix A

ENG4111/4112 Research Project

Project Specification

For:	Iman Farahbakhsh
Title:	Finite Element Modelling of Hybrid Sandwich Panels in Strand7
Major:	Civil Engineering
Supervisor:	Associate Professor Yan Zhuge
Enrolment:	ENG4111 – EXT S1, 2016 ENG4112 – EXT S2, 2016
Project Aim:	To analyse the behaviour of new hybrid sandwich panels by Finite Element Modelling in Strand7
Programme:	Issue A, 16th March 2016

1. Develop the finite element model of typical sandwich panels in Strand7
2. Develop the finite element model of new Hybrid sandwich panel with Jute and hemp intermediate layer for both medium and large sizes.
3. Produce load versus defection graph using acquired data from Strand7 for each specimen and compare the acquired data from Strand7 with the experimental data
4. Display the stress distribution in each specimen (medium and large)
5. Compare the behaviour of the panels under a particular load illustrating the effect of using NFRP as intermediate layer
6. Undertake the parametric study using various natural fibres and compare the results

If time permits:

7. Make recommendations on the optimum thickness and type of the NFRP intermediate layer to be used in sandwich panels.
8. Use ANSYS to validate results from Strand7 and also, compare the method and difficulty level for both FEM software.

Project plan

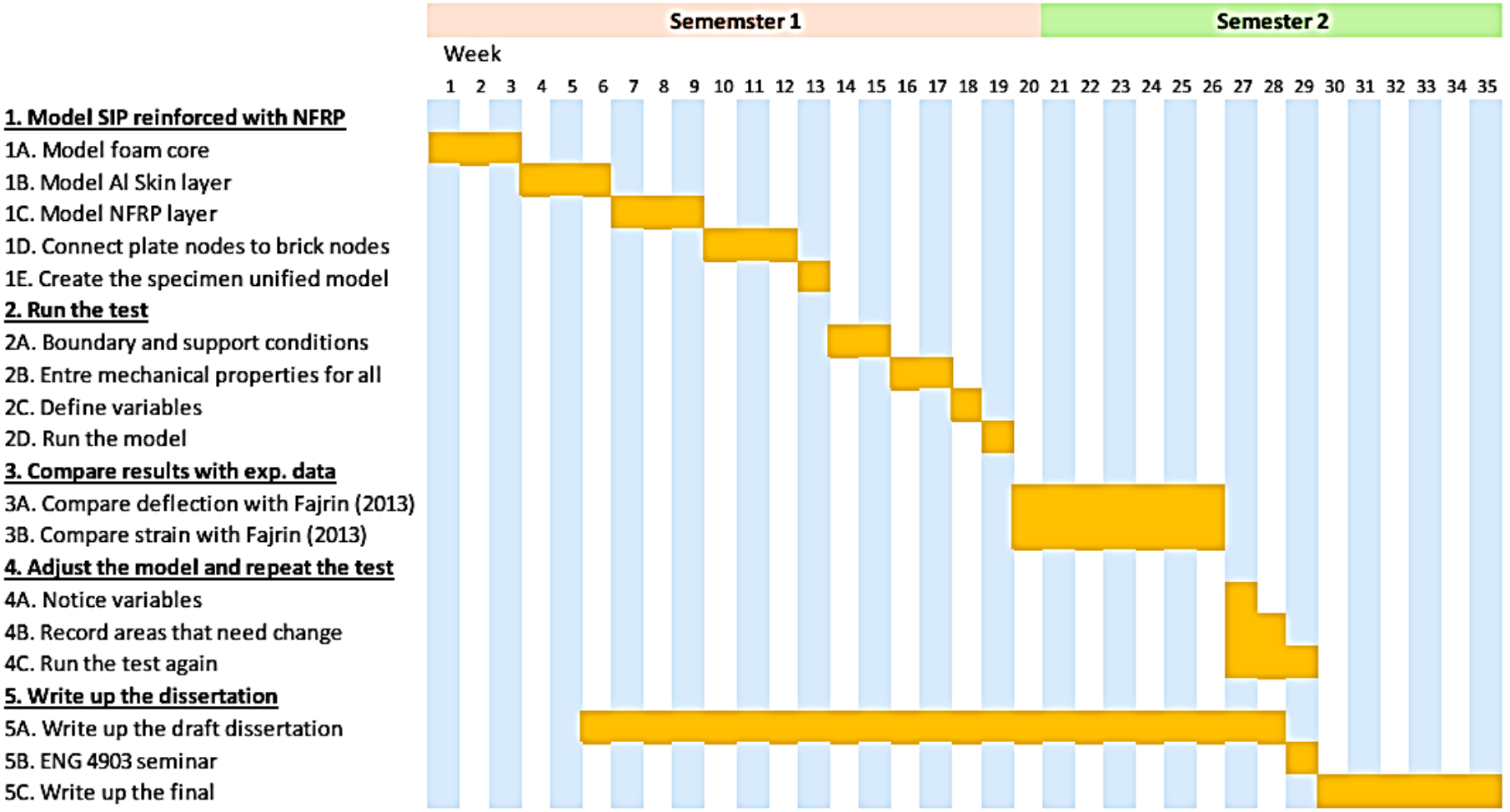

Project Resources

- Strand7 FEM software
- ANSYS FEM software
- Experimental data (Fajrin 2013)
- Various papers and books for obtaining mechanical properties of aluminium, EPS, jute, hemp and other intermediate layers.

All resources are available by date. Student version of Strand7 can be purchased from Strand7 website. The main paper is supplied by the supervisor and required data being collected from various reliable journals and books available online or at the university's library. It should be taken into account that finding properties of natural fibres for entry into Strand7 would be challenging as they are orthotropic material. However, there are various reliable publications on the internet and library that ease the process. Properties of aluminium, EPS and jute are available currently while finding hemp mechanical properties is the next step to be achieved from online books and journals.

Appendix B

Theoretical deflection of a hybrid sandwich panel example by Dr. Fajrin:

Hybrid sandwich panel's cross section:

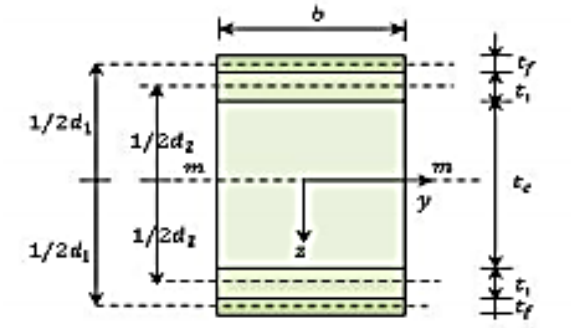

Data:

t_f = 0,5 mm
t_i = 3 mm
t_c = 15 mm
E_f = 68200 MPa
E_i = 4502 MPa
E_c = 7.25 MPa
b = 50 mm
L = 450 mm
v_c = 0.35
v_f = 0.33
v_i = 0.235

Calculation:

d_2 = 15 + (2*0.5*3) = 18 mm

Flexural rigidity of the hybrid sandwich panel is given by Equation 3.51 in C

$$(EI)_{eq} = E_f\left[\frac{bt_f^3}{6} + \frac{bt_f d_1^2}{2}\right] + E_i\left[\frac{bt_i^3}{6} + \frac{bt_i d_2^2}{2}\right] + E_c\frac{bt_c^3}{12}$$

- Flexural rigidity of the face:

$$= 68200\left[\frac{50 * 0.5^3}{6} + \frac{50 * 0.5 * 21.5^2}{2}\right]$$

$$= 395139167\ \text{Nmm}^2$$

- Flexural rigidity of the intermediate layer:

$$= 4502\left[\frac{50 * 3^3}{6} + \frac{50 * 3 * 18^2}{2}\right]$$

$$= 110411550\ \text{Nmm}^2$$

- Flexural rigidity of the core:

$$= 7.25 * \frac{50 * 15^3}{12}$$

$$= 101949 \text{ Nmm}^2$$

Total flexural rigidity:

$$(EI)_{eq} = 395139167 + 110411550 + 101949$$

$$= 504652670 \text{ Nmm}^2$$

Total deflection is defined by Equation 5.10 in Chapter 5:

$$\delta = \frac{23 \text{ PL}^3}{1296(\text{EI})_{eq}} + \frac{\text{PL}}{6(\text{AG})_{eq}}$$

For the calculation of deflection, P = 1/2 P. Hence, when checking the deflection at the load (P) of 200 N, the value of P is equal to 100 N.

- Deflection due flexure:

$$= \frac{23 * 100 * 450^3}{1296 * 504652670}$$

$$= 0.32 \text{ mm}$$

- Deflection due shear:

$$= \frac{100 * 450}{6 * 50 * 18 * 2.69}$$

$$= 3.10 \text{ mm}$$

Finally, the total deflection is:

$$\delta_{total} = 0.32 + 2.48$$

$$= 3.42 \text{ mm}$$

Appendix C

Load versus Strain graph for medium scale specimens in experimental study:

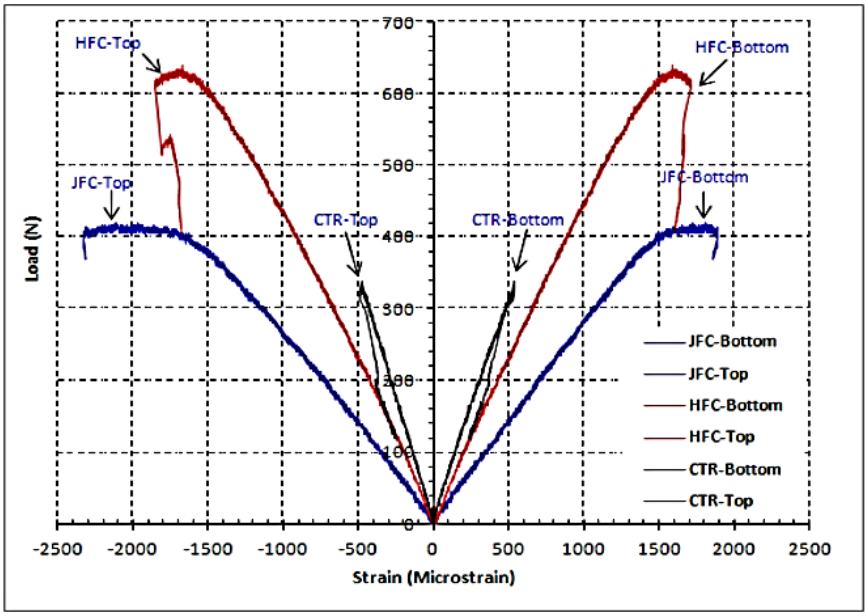

Load versus Strain graph for large scale specimens in experimental study:

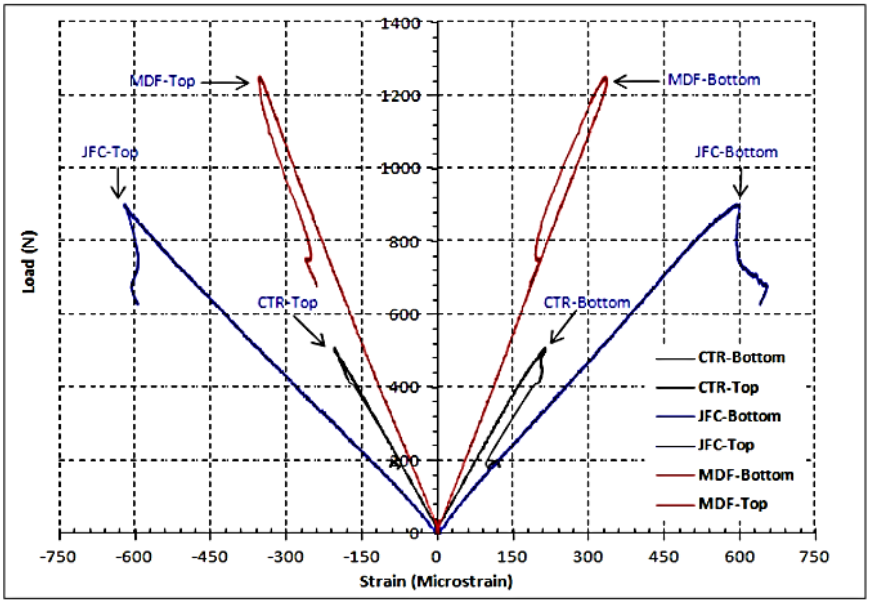

Appendix D

Stress distribution of all specimens

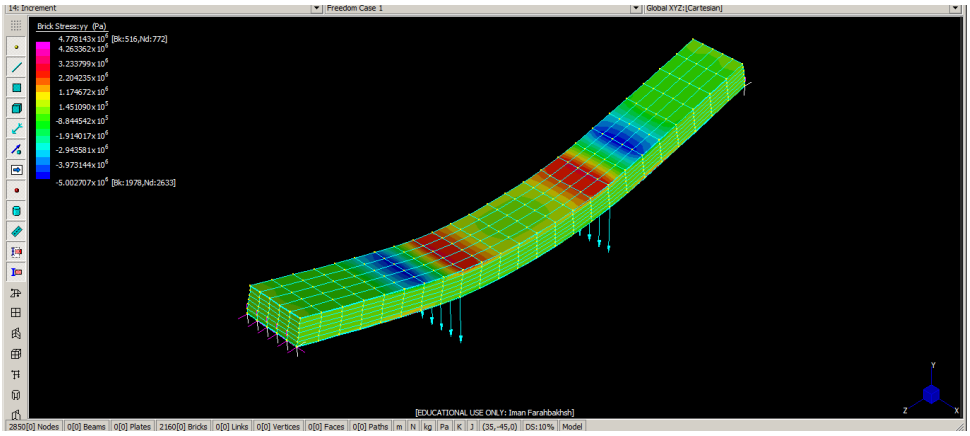

Figure D. 1: CTR-SP Shear Stress distribution

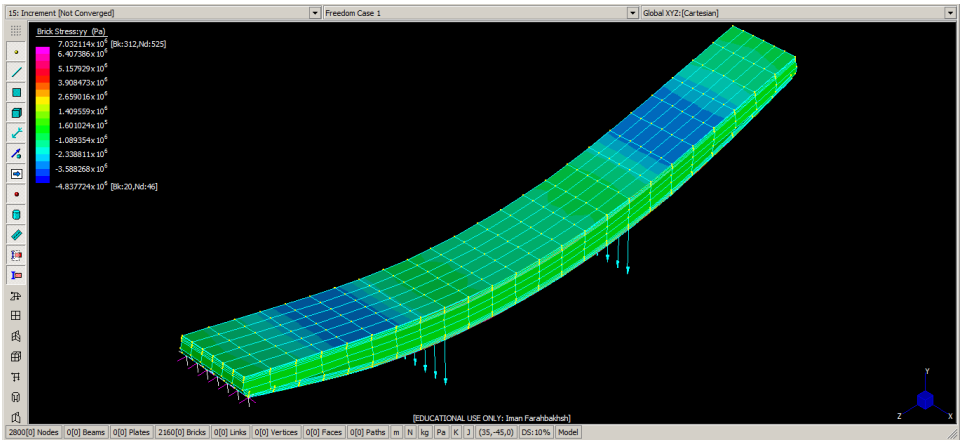

Figure D. 2: JFC-SP Shear Stress distribution

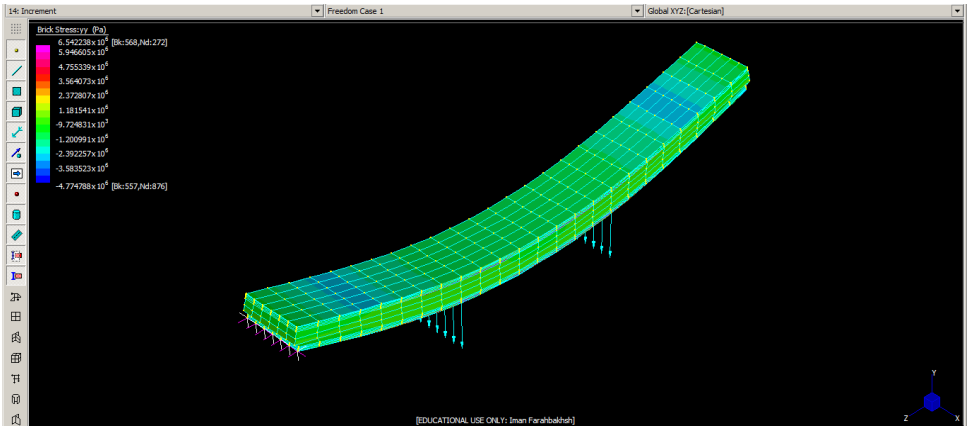

Figure D. 3: HFC-SP Shear Stress distribution

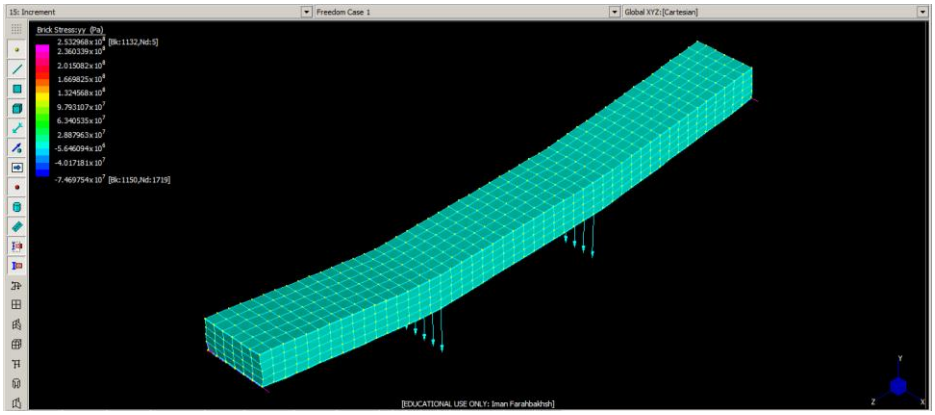

Figure D. 4:CTR-SIP Shear Stress distribution

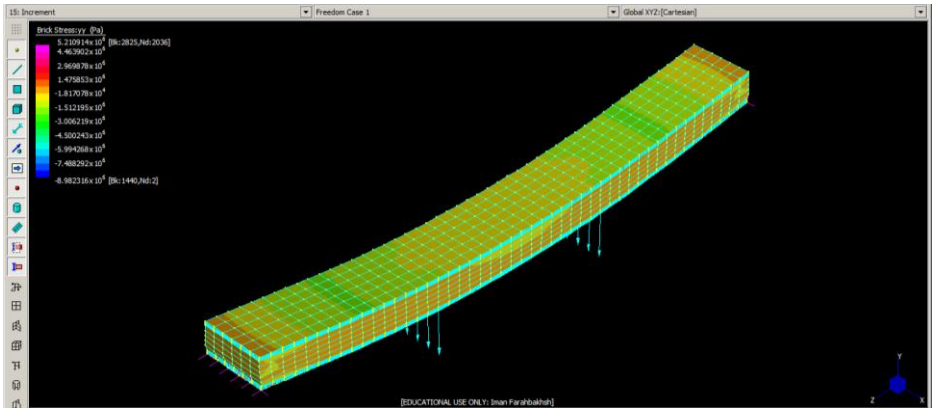

Figure D. 5:JFC-SIP Shear Stress distribution

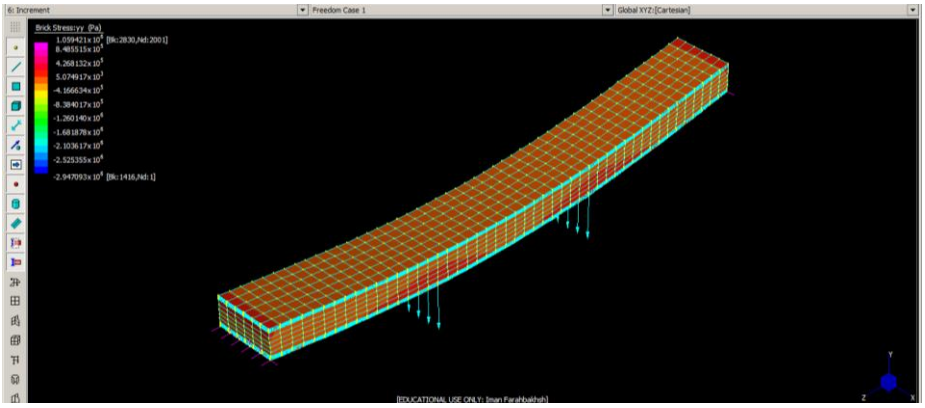

Figure D. 6: MDF-SIP Shear stress distribution

Appendix E

Load increments of specimens used in this project:

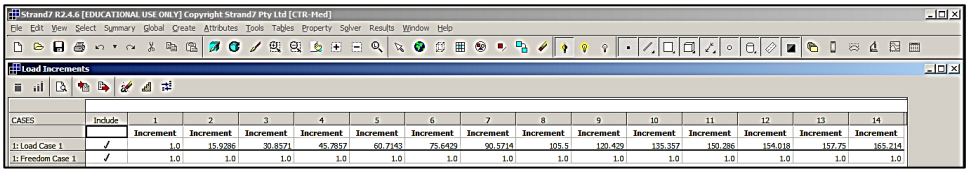

Figure E. 1: Load increments used in CTR-SP

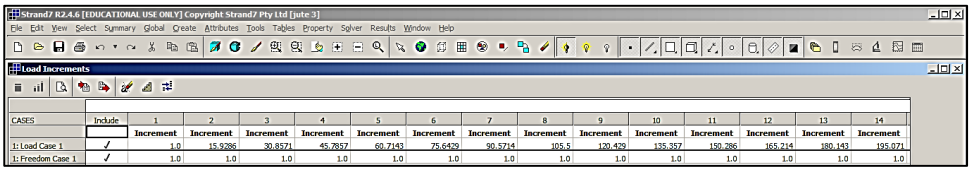

Figure E. 2: Load increments used in JFC-SP

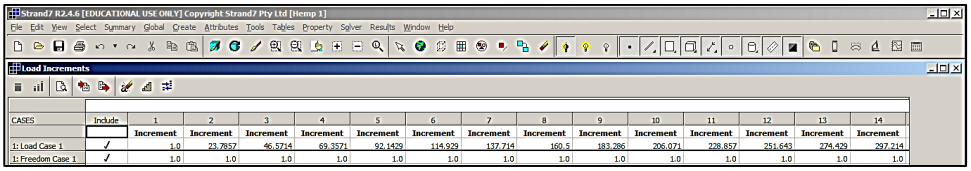

Figure E. 3: Load increments used in HFC-SP

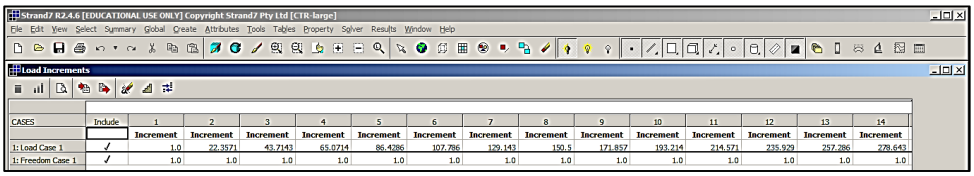

Figure E. 4: Load increments used in CTR-SIP

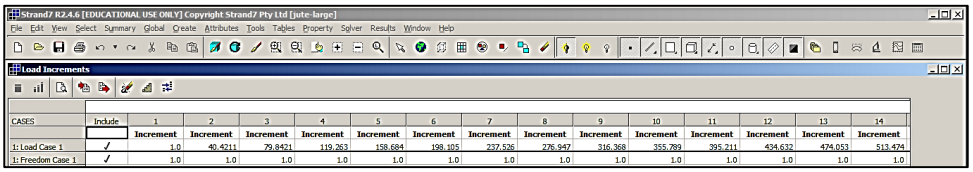

Figure E. 5: Load increments used in JFC-SIP

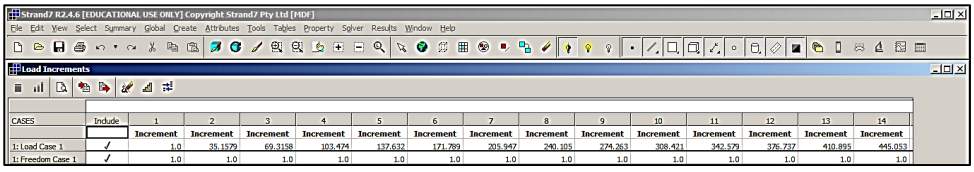

Figure E. 6: Load increments used in CTR-SP